

1 **Late Triassic tectonic inversion in the upper Yangtze Block: insights from detrital**
2 **zircon U–Pb geochronology from southwestern Sichuan Basin**

3
4 Zhaokun Yan^{1,2,3}, Yuntao Tian^{3,4*}, Rui Li³, Pieter Vermeesch³, Xilin Sun⁵, Yong Li², Martin Rittner³,
5 Andrew Carter⁶, Chongjian Shao², Hu Huang², Xiangtian Ji²

6
7 ¹ *State Key Laboratory of Mineral Deposits Research, School of Earth Sciences and Engineering,*
8 *Nanjing University, Nanjing 210023, China*

9 ² *State Key Laboratory of Oil and Gas Reservoir Geology and Exploitation (Chengdu University of*
10 *Technology), Sichuan Chengdu, 610059, China*

11 ³ *Department of Earth Sciences, University College London, London, WC1E 6BT, UK*

12 ⁴ *School of Earth Sciences and Engineering, Sun Yat-sen University, Guangzhou, 510275, China*

13 ⁵ *Cluster Geology and Geochemistry, VU University Amsterdam, De Boelelaan 1085, 1081 HV*
14 *Amsterdam, The Netherlands*

15 ⁶ *Department of Earth and Planetary Science, Birkbeck University of London, Malet Street,*
16 *Bloomsbury, London WC1E 7HX, UK*

17
18
19 *Corresponding author:

20 Yuntao Tian

21 School of Earth Sciences and Engineering

22 Sun Yat-sen University

23 Guangzhou, China

24 Email: tianyuntao@mail.sysu.edu.cn

25
26
27 **ABSTRACT**

28 The Sichuan Basin and the Songpan-Ganzi terrane, separated by the Longmen Shan fold-and-thrust belt
29 (the eastern margin of the Tibetan Plateau), are two main Triassic depositional centers, south of the
30 Qinling-Dabie orogen. Closure of the Paleo-Tethys Ocean during the Middle – Late Triassic saw the
31 Sichuan Basin region, located at the western margin of the Yangtze Block, transition from a passive
32 continental margin into a foreland basin. In the meantime, the Songpan-Granze terrane evolved from a
33 marine turbidite basin into a fold-and-thrust belt. To understand if and how the regional sediment routing
34 system adjusted to these tectonic changes, we applied detrital zircon U-Pb analyses to representative
35 stratigraphic samples from the southwestern edge of the Sichuan Basin to monitor sediment provenance.
36 Integration of the results with paleocurrent and published detrital zircon data from other parts of the basin
37 identified a marked change in provenance between Early-Middle Triassic samples, dominated by
38 Neoproterozoic (~700-900Ma) zircons sourced mainly from the northern Kangdian basement to the south,
39 and Late Triassic sandstones that contain a more diverse range of zircon ages, sourced from the Qinling,
40 Longmen Shan and Songpan-Ganzi terrane. This change reflects a major drainage adjustment in response
41 to the Late Triassic closure of the Paleo-Tethys Ocean and significant shortening in the Longmen Shan
42 thrust belt and the eastern Songpan-Ganzi terrane. Further, at late Triassic time, the northern Kangdian

43 basement was inverted from uplift and erosion into subsidence. Considering the eastward paleocurrent
44 and depocenter geometry of the upper Triassic deposits, the subsidence of the northern Kangdian
45 basement probably resulted from the eastward shortening and loading of the Songpan-Ganze terrane over
46 the western margin of the Yangtze Block in response to the Late Triassic collision between Yangtze
47 Block, Yidun arc and Qiangtang Terrane along the Ganzi-Litang and Jinshajiang sutures.

50 INTRODUCTION

51 The Sichuan Basin, the western margin of the Yangtze block, shares common borders with four
52 major tectonic terrains – the Qinling-Dabie orogen to the north, the Songpan-Ganzi terrane (i.e. the
53 eastern Tibetan Plateau) to the west, the Yidun Arc to the south and the eastern Sichuan fold-and-thrust
54 belt to the east (Fig. 1). Numerous structural, geochronological, and sedimentary studies suggested that
55 these areas had experienced a significant phase of crustal shortening and rock exhumation during the
56 Triassic closure of the Paleo-Tethys Ocean (Burchfiel *et al.*, 1995; Zhang *et al.*, 1995; Yin, 1996; Meng
57 & Zhang, 2000; Li *et al.*, 2003a; Wang *et al.*, 2005; Jia *et al.*, 2006), and the Sichuan Basin changed from
58 a passive continental margin to a foreland basin.

59 In the context of these changes, the provenance of sediments deposited in the Sichuan Basin have
60 seen extensive study, much based on detrital zircon U-Pb geochronology work (Deng *et al.*, 2008; Chen,
61 2011; Luo *et al.*, 2014; Zhang *et al.*, 2015; Li *et al.*, 2016; Shao *et al.*, 2016; Zhu *et al.*, 2017). Results
62 from previous work suggest that the sediments in the basin were mainly sourced from the Qinling-Dabie
63 orogen, to the north, and the Longmen Shan thrust belt and the Songpan-Ganzi terrane to the west.
64 However, most of those previous studies focused on the post-Late Triassic foreland basin sediments in
65 the western and northern part of the Sichuan Basin (Fig.1). The provenance of pre-Late Triassic passive
66 continental margin clasts remains elusive. Constraining the provenance of the sediments deposited before
67 and after the Late Triassic tectonic inversion could provide significant insights into whether the sediment
68 routing system into the basin had significantly changed by the inversion event.

69 Previous sedimentary and stratigraphic studies suggested that during the Early – Middle Triassic,
70 the southwestern basin margin was bounded by a highland, as indicated by a lateral sedimentary facies
71 transition from clastic to carbonate away from the basin edge to interior (Liu & Tong, 2001; Long *et al.*,
72 2011; Zhao *et al.*, 2012; Tan *et al.*, 2014; Wei *et al.*, 2014). The highland consists of Neoproterozoic
73 basement and is referred to as the Kangdian basement (named as the Kangdian Oldland or Kangdian
74 Axis by Chinese researchers) (Li, 1963; Luo, 1983; Wang *et al.*, 1983; Dai *et al.*, 2012; Tan *et al.*, 2013)
75 (Fig. 1). However, the lithology of Late Triassic sediments in the southern Sichuan Basin is similar to
76 those in other parts of the basin, sourced mainly from the Longmen Shan thrust belt and the Qinling-
77 Dabie orogen. This implies that a significant change in sediment provenance might have occurred during
78 the Late Triassic basin inversion. To test this, we applied detrital zircon geochronology to nine Early-
79 Late Triassic sandstone and one volcanic tuff outcrop samples collected from the southwestern part of
80 the Sichuan Basin. The results are interpreted together with previously mapped stratigraphic correlations
81 and paleocurrent data, so as to constrain the paleogeographic evolution of the southwestern margin of
82 the Sichuan Basin during Early-Late Triassic time, and to test if the crustal shortening and rock
83 exhumation during the Triassic had influenced the sedimentary delivery network in the basin margin.

85 **GEOLOGICAL SETTING**

86 The southwestern part of Sichuan Basin is bounded by the Kangdian basement to the south and
87 Songpan-Ganzi terrane and Longmen Shan to the west (Figs. 1, 2). The Triassic regional tectonism and
88 geological evolution of these major terranes is summarized below.
89

90 **Regional Tectonism**

91 Triassic evolution of the Sichuan Basin and surrounding regions was controlled by the Middle
92 - Late Triassic closure of the Paleo-Tethys Ocean along the Mianlue suture, forming the Qinling-
93 Dabie orogen (e.g., Zhang, *et al.*, 1995; Yin, 1996; Meng, & Zhang, 2000; Li, *et al.*, 2003), and the
94 Litang and Jinshajiang sutures north and south of the Yidun Arc (Fig. 3, e.g., Reid *et al.*, 2005; Roger
95 *et al.*, 2008; Pullen *et al.*, 2008; Roger *et al.*, 2010; Yuan *et al.*, 2010; Wang *et al.*, 2013). During the
96 process, margins of the Sichuan Basin, especially the Longmen Shan and Songpan-Ganzi turbidite
97 terrane to the west, has been significantly shortened (e.g., Huang *et al.*, 2003; Yan *et al.*, 2011; Weller
98 *et al.*, 2013; Zheng *et al.*, 2016), inducing several kilometers of flexural subsidence along the margins
99 of the Sichuan Basin (e.g., Guo *et al.*, 1996; Li, *et al.*, 2003; Meng *et al.*, 2005). In Cenozoic time,
100 margins of the Sichuan Basin were reactivated by the Indo-Asian collision and the subsequent
101 outward growth of the Tibetan Plateau (Liu-Zeng *et al.*, 2008; Wang *et al.*, 2012; Tian *et al.*, 2012,
102 2013).

103 **Sichuan Basin**

104 The Phanerozoic geological evolution of the Sichuan Basin can be divided into three major stages:
105 a passive margin stage characterized by platform carbonates during Paleozoic to Middle Triassic time
106 (Xu *et al.*, 1997), a Late Triassic foreland basin characterized predominantly by continental siliciclastic
107 sedimentation and a terrestrial foreland basin or intracratonic stage from the Jurassic to Quaternary (Li
108 *et al.*, 2003a). The eastern and central Sichuan Basin experienced a prolonged phase of denudation since
109 late Cretaceous time, as shown by thermochronological studies (Tian *et al.*, 2012). In this study, we focus
110 on the Triassic strata in the southwest that consists of Feixianguan, Jialingjiang, Leikoupo, Maantang,
111 Xiaotangzi and Xujiache Formations, from bottom to top (Fig. 3).

112 (1) The marine Feixianguan Formation is widely distributed in the Sichuan Basin, but shows marked
113 lateral lithofacies variations. The formation consists of purple shale and sandy shale, interbedded with
114 grey limestone, oolitic limestone, marl and sandstone in the western Sichuan Basin, but changes into
115 limestone toward the eastern basin (BGMRS, 1997). The biostratigraphic age of the formation is early-
116 early Triassic (BGMRS, 1997). Several volcanic ash beds at the bottom of the formation compare well
117 with the ash sequence of the Global Stratotype Section (Meishan section) (Huang *et al.*, 2017) that has
118 ash beds (~252Ma) (Burgess *et al.*, 2014) providing a quantitative constraint for the age of the
119 Feixianguan Formation. The isopach map of this formation shows a depocenter located in the center of
120 the Sichuan basin (Fig. 4a).

121 (2) The marine Jialingjiang Formation conformably overlies the Feixianguan Formation, and is
122 mainly composed of limestone and dolomite (BGMRS, 1997). In the formation, Late-Early Triassic
123 bivalves, ammonites, foraminiferas and conodonts have been discovered (BGMRS, 1997). The top of
124 the formation is marked by a widespread thin layer (the thickness is 10s cm – 1 m) of altered tuff (named
125 as “green-bean rocks” in early Chinese literature) (Zhu & Wang, 1986), that has been dated to ~247 Ma

126 by ID-TIMS, LA-ICP-MS or CA-TIMS (Ovtcharova *et al.*, 2006; Xie *et al.*, 2013; Lehrmann *et al.*, 2015).

127 (3) The marine Leikoupo Formation mainly consists of dolomite and argillaceous dolomite,
128 interbedded with limestone and gypsum layers (BGMRSF, 1997). It contains Middle Triassic bivalves
129 and ammonites such as *Progonoceras*, *Beyrichites* (BGMRSF, 1997). The boundary between the
130 Leikoupo and underlying Jialingjiang formations is the altered tuff. The isopach map of this formation
131 shows a depocenter located in the center of the Sichuan basin (Fig. 4b).

132 (4) The marine Maantang Formation, distributed in the western Sichuan Basin, mainly consists of
133 marine black mudstone and shale interbedded with siltstone, marl, oolitic and bioclastic limestones and
134 sponge reefs (BGMRSF, 1997; Li *et al.*, 2003a). It is regarded as Carnian in age on the basis of its fossil
135 content (Shi *et al.*, 2016). The Kuahongdong Formation represents equivalent coeval strata in the
136 southwestern margin of the Sichuan Basin, and is composed of conglomerate, mudstone, argillaceous
137 limestone and argillaceous dolomite (BGMRSF, 1997).

138 (5) The Xiaotangzi Formation, is composed of black marine shale, mudstone, quartz arenite, lithic
139 arenite and siltstone, and can be divided into three parts: a lower part, composed of black shale
140 interbedded with quartz arenite, a middle part, composed of lithic arenite and black shale, and an upper
141 part, composed of arkose. The formation coarsens upwards and is thought to represent a transition from
142 marine shelf to delta environments. It has an early Norian age based on its fossil content (Li *et al.*, 2003a).

143 (6) The Xujiuhe Formation conformably overlies the Xiaotangzi Formation in the western Sichuan
144 Basin, and unconformably overlies Middle Triassic limestone of the Leikoupo Formation in the central
145 and eastern Sichuan Basin. Widely distributed in the Sichuan Basin, the lithology and facies of the
146 formation changes from coarse-grained sediments, including alluvial conglomerate bodies along the front
147 of the Longmen Shan thrust belt, to fine-grained lacustrine deposits in the basin interior. Two depocenters,
148 located in front of the middle segment of the Longmen Shan thrust belt and areas to the south, have
149 developed (Fig. 4c). Depositional age of the formation is late Norian to Rhaetian based on the fossil
150 content (WGCMSPIB, 1984; Li *et al.*, 2003a).

151 Previous sedimentary studies suggested that the clastic deposits of Feixianguan, Jialingjiang and
152 Leikoupo formations in the southwestern margin of the Sichuan Basin were sourced from the south, as
153 shown by a facies transition from clastic to carbonate deposits from the margin to the interior of the basin
154 (Feng *et al.*, 1997; Tan *et al.*, 2014; Sun *et al.*, 2015). The Kangdian basement might be the source of
155 Upper Triassic sediments, as suggested by studies on the detrital mineral assemblage, sedimentary
156 system and conglomerate composition (Xie *et al.*, 2006; Jiang *et al.*, 2007; Shi *et al.*, 2010). However,
157 nonmarine Upper Triassic sediments unconformably overlie rocks of the Kangdian basement (BGMRSF,
158 1991) indicating that the region was likely an area of deposition rather than erosion (Liu & Tong, 2001;
159 Yi *et al.*, 2014).

160 **Kangdian Basement**

161 The Kangdian basement forms the western margin of the Yangtze Block and extends for over 700
162 km from Kangding in the north to Yuanmou in the south (Zhou *et al.*, 2002a; Zhu *et al.*, 2011). It is
163 located in the western margin of the Yangtze Block (Fig. 1), and it mainly consists of Precambrian
164 basement. It is overlain by marine Paleozoic cover and locally by Upper Triassic to Cenozoic terrestrial
165 sediments (BGMRSF, 1991). Extensive Neoproterozoic magmatism (mainly ~740–870 Ma) is probably
166 associated with the breakup of the supercontinent Rodinia due to a mantle plume (Li *et al.*, 2003b), or
167 the subduction of the Mozambique oceanic slab beneath the western margin of the Yangtze Block (Zhao
168 & Zhou, 2007; Sun *et al.*, 2009).

169 There is a debate on the geological evolution of Kangdian area throughout the Paleozoic and
170 Mesozoic. One school of thought is that the Kangdian area was a region of erosion between the
171 Ordovician and Carboniferous (Li, 1963), followed by a rift subsidence stage from Late Permian to
172 Jurassic (Luo, 1983; Guo et al., 1996). A different point of view is that the Paleozoic - Mesozoic
173 geological evolution of the region can be divided into three stages: a stable marine platform from the
174 Cambrian to Early Permian, an uplift stage affected by Emeishan mantle plume from Late Permian to
175 Middle Triassic, and transtensional subsidence during the Late Triassic and Jurassic (Chen et al., 1987;
176 Feng et al., 1994; Wang et al., 1994; He et al., 2003; Chen et al., 2011).

177 Longmen Shan

178 The Longmen Shan is approximately 500km long and 30-50km wide, and defines a major part of
179 the highly dissected eastern margin of Tibetan Plateau. Neoproterozoic lithologies, surrounded by
180 Paleozoic sedimentary strata, crop out in the Longmen Shan. Zircon U-Pb analyses of the Neoproterozoic
181 basement rocks yielded mainly ages of 770-890 Ma (Fu et al., 2013), which is similar in age and
182 petrology of Neoproterozoic magmatism of Kangdian Basement.

183 The Longmen Shan thrust belt experienced three phases of intra-continental orogenic shortening in
184 the early Mesozoic and late Cenozoic. Various lines of geochronological and structural evidence have
185 been reported for the late Triassic formation of the Longmen Shan thrust belt (Huang et al., 2003; Yan et
186 al., 2011; Weller et al., 2013). The second phase of deformation is characterized by contemporaneous
187 hinterland-ward shearing and foreland-ward thrusting in the back and front sides of the Longmen Shan
188 thrust belt (e.g., Tian et al., 2016). Synkinematic mica $^{40}\text{Ar}/^{39}\text{Ar}$ geochronological analyses suggest the
189 deformation is of late Cretaceous – early Paleogene time belt (Tian et al., 2016). The last phase of
190 deformation has occurred during the late Cenozoic. During this phase, pre-existing structures were
191 reactivated by the eastward growth of the Tibetan Plateau (e.g. Wang et al., 2012; Tian et al., 2013).

192 Songpan-Ganzi terrane

193 Songpan-Ganzi terrane currently form a triangular fold belt wedged between the North China block,
194 Yangtze block, and Qaidam block (Fig. 1). More than 80% of the Songpan-Ganzi terrane is covered by
195 thick Triassic turbidites, which was mainly sourced from the Qinling-Dabie orogen to the northeast
196 and terranes to the north (Enkelmann et al., 2007; Ding et al., 2013). By latest Triassic, the Songpan
197 - Ganzi basin had shallowed, as documented by coeval coal-bearing clastic deposits (BGMRSP,
198 1991; Chang, 2000). In response to the closure of the paleo-Tethys Ocean the flysch basin evolved
199 into a fold belt during late Triassic time (Xu et al., 1992; Roger et al., 2011). Jurassic – Cenozoic
200 deposits, have been recently reported in the western part of the terrane (Ding et al., 2013).

201 The Songpan-Ganzi terrane was intruded by Late Triassic–Jurassic granitoids (Roger et al.,
202 2011). with ages in the range 228 - 153 Ma (Roger, et al., 2004; Zhang, et al., 2006; Xiao, et al.,
203 2007; Zhang, et al., 2007; Weislogel, 2008; Yuan, et al., 2010). Metamorphic grade varies across
204 the Songpan-Ganzi terrane. In general, the metamorphic overprint is relatively strong along the
205 terrane margins where mudstones were metamorphosed to phyllite, but weak within the interior
206 (Chang, 2000).

207

208 PREVIOUS DETRITAL ZIRCON STUDIES

209 Over the past decade, the provenance of the Upper Triassic clastic sediments in the Sichuan Basin
210 has been intensively studied, especially by detrital zircon geochronology (Fig. 1), but this has led to
211 conflicting conclusions. Deng *et al.* (2008) reported age spectra of four Upper Triassic sandstone samples
212 from the western Sichuan Basin and the eastern Songpan-Ganzi terrane, and suggested that the Upper
213 Triassic Xujiahe Formation was sourced from the Songpan-Ganzi terrane and Longmen Shan thrust belt.
214 By contrast the study of Chen (2011) based in the northern and western parts of the Sichuan Basin
215 indicated that the Qinling orogen to the north was the main source of sediments. Recently work by Luo
216 *et al.* (2014), Zhang *et al.*, (2015) and Shao *et al.*, (2016), suggest that the Longmen Shan thrust belt and
217 the Songpan-Ganzi terrane in the west and the Qinling-Dabie orogen in the north were the source of the
218 Upper Triassic sediments in the western and northern Sichuan Basin, respectively. Zhang *et al.* (2015)
219 and Shao *et al.* (2016) also indicated the minor role of the north Yangtze Block in supplying sediments
220 to the northern Sichuan Basin. Shao *et al.* (2016) suggested that sediments of the western, southern and
221 eastern parts of basin shared the same sources that include the southern North China Block and Qinling
222 orogen, and the eastern Songpan-Ganzi terrane via the Longmen Shan thrust belt. Zhu *et al.* (2017)
223 reported age spectra of four Middle-Upper Triassic sandstone samples from the southwestern Sichuan
224 Basin, and suggested that Middle Triassic sediments mainly sourced from the Kangdian basement and
225 Emeishan Large Igneous Province to the south, whereas Upper Triassic sediments mainly from the
226 Songpan-Ganzi terrane and Yidun Arc to the west with a minor component from the Qinling orogen to
227 the north and Jiangnan Xuefeng thrust belt (southeastern Yangtze Block) to the east. Importantly, all
228 these previous studies focused on the Upper Triassic; little is known about the source of the Lower
229 Triassic clastic rocks. One of the core aims of this study therefore, is to try and resolve the ongoing debate
230 about the sources of the Triassic sediments.

231 SAMPLING AND ANALYTICAL METHODS

232 Ten samples were collected from the Longcanggou, Longmendong and Chuanzhu sections in the
233 southwestern part of the Sichuan Basin. The sections expose all lithologic formations of the Triassic
234 sediments (Figs. 5 and 6). Details of the stratigraphy and sedimentology features of the sections are
235 provided in the supplementary material. The samples include two samples from the Early Triassic
236 Feixianguan (T_{1f}) and Jialingjiang Formation (T_{1j}), one volcanic tuff sample from the boundary between
237 the Jialingjiang Formation (T_{1j}) and Leikoupo (T_{2l}), two samples from the Middle Triassic Leikoupo
238 Formation (T_{2l}) and five samples from the Upper Triassic Maantang (T_{3m}) Xiaotangzi (T_{3xt}) and Xujiahe
239 formations (T_{3x}) (Figs. 5 and 6).

240 Where possible, more than 100 U/Pb ages were derived by LA-ICP-MS using the facilities at the
241 London Geochronology Centre, University College London, which include a New Wave NWR193
242 excimer laser ablation system and an Agilent 7700x quadrupole mass spectrometer. The laser was set to
243 produce ~2.5 J/cm² energy density at 8 Hz repetition rate for 25 seconds. The spot diameter was set to
244 25 µm for all analyses. Repeated measurements of internal U/Pb age standard Plešovice [TIMS reference
245 age of 337.13 ± 0.37 Ma (Sláma *et al.*, 2008)] and NIST-610 silicate glass (Jochum *et al.*, 2011) were
246 used to correct for instrumental mass bias and laser-pit-depth-dependent isotopic fractionation. GJ-1
247 (Jackson *et al.*, 2004) and 91500 zircon (Wiedenbeck *et al.*, 2004) were used as external standards. Data
248 reduction was processed using the GLITTER software package (Griffin *et al.*, 2008).

249 The paleocurrent data were determined in the field based on cross-bedding and ripples in sandstone

250 beds. The orientations of trough cross laminations were measured using the method described by
251 DeCelles *et al.* (1983).

252 RESULTS

253 Paleocurrent

254 Paleocurrent data were collected from 7 sites, as summarized in the Fig. 2. The paleocurrent in the
255 Feixianguan formation, measured in the Longcanggou section (L01), is eastward (Fig. 5), as determined
256 from cross-bedding in sandstone beds. The results, derived from cross-bedding and current ripples in
257 sandstone in the Longcanggou (L02), Chuanzhu (C01, C02) and Hanyuan areas (YD01, SQ02, HY01),
258 indicates eastward and southeastward paleocurrent directions for the Xiaotangzi and Xujiuhe Formations
259 (Fig. 5).

260 Zircon U-Pb isotopic results

261 In total, 1132 detrital zircons from nine detrital samples analyzed in this study. The U–Pb data for
262 each sample are presented in supplementary Table. As with convention, we only consider U-Pb ages that
263 were no more than 15% discordant or 5% reverse discordant. The data are visualized as kernel density
264 estimate (KDE, Vermeesch, 2012) plots.

265 *Altered tuff*

266 Sample SZ02 (102°51'42.92" E, 29°40'47.12"N) of the altered tuff was collected from the boundary
267 between the Leikoupo and Jialingjiang formations in the Longcanggou section. 30 of 34 analyses yielded
268 concordant ages. The data are concordant within analytical error and define a weighted mean $^{206}\text{Pb}/^{238}\text{Pb}$
269 age of 246.5 ± 1.7 Ma (n=26) (Fig. 7), which is similar to the previous studies in other sites of the Yangtze
270 Block (Ovtcharova *et al.*, 2006; Xie *et al.*, 2013; Lehrmann *et al.*, 2015). The complete U–Pb isotopic
271 data and calculated dates are presented in supplementary Table 1.

272 *Lower Triassic Feixianguan and Jialingjiang Formations*

273 Sample LCG01 (102°51'42.92" E, 29°40'47.12"N), a grey-green fine-grained sandstone, was
274 collected from the Feixianguan Formation in the Longcanggou section (Fig. 6). ninety-nine of 156
275 analyses yielded concordant ages, which exhibit a wide spectrum from ca. 243 ± 3 Ma to 2.4 Ga. The KDE
276 plot of this sample shows a major peak at ~800 Ma, and three minor peaks at ~248 Ma, ~510 Ma and
277 ~950 Ma (Fig. 8a).

278 Sample LMD02 (103°25'5.73" E, 29°34'46.76"N), a grey-purple coarse sandstone, was collected
279 from the Jialingjiang Formation in Longmendong section (Fig. 6). Among 129 analyses, 123 analyses
280 yield concordant ages. Nearly all ages are between 730 - 880 Ma, showing a dominant peak at ~800 Ma
281 in the KDE plot (Fig. 8b).

282 *Middle Triassic Leikoupo Formation*

283 Two samples (grey coarse sandstone), LCG03 (102°51'35.19" E, 29°40'51.35"N) and LCG04

284 (102°51'35.05" E, 29°40'51.18"N), were collected from the Leikoupo Formation in Longcanggou section
285 (Fig. 6). one hundred and thirty-six out of 153 single zircon dates of the sample LCG03 are concordant.
286 The ages exhibit a wide range from ca. 242±3Ma to 2.5Ga, with 74% lying between 730 Ma and 880 Ma,
287 showing a dominant mode at ~800Ma (Fig. 8c), similar to the lower sample LMD02 from Jialingjiang
288 Formation.

289 One hundred and fifty-two out of 157 single zircon dates of the sample LCG04 are concordant. The
290 ages exhibit a wide range from ca. 233±3Ma to 3.0Ga; but most of them fall between 230 Ma to 1050
291 Ma (89%). The KDE plot of the sample shows a mode at ~800Ma, and three minor peaks at ~248Ma,
292 ~510Ma and ~950Ma (Fig. 8d).

293 *Upper Triassic Maantang and Xujiahe Formation*

294 Two samples (grey sandstone), LCG05 (102°51'34.05"E, 29°40'51.18"N) and LCG06
295 (102°51'34.05"E, 29°40'51.18"N), were collected from the Maantang Formation and the upper part of
296 Xujiahe Formation in the Longcanggou section (Fig. 6). One hundred and forty-nine of 154 single zircon
297 dates of the sample LCG05 are concordant. Most ages cluster at ~1800 Ma, with minor peaks at ~250
298 Ma, ~800 Ma and ~2500 Ma (Fig. 8e). Their age spectra are significantly different from the lower ones
299 (Fig. 8a-d). Ninety-nine of 110 single zircon dates of the upper Triassic sample LCG06 are concordant.
300 The KDE plot shows five peaks at ~246 Ma, ~440 Ma, ~758 Ma, ~1870 Ma and ~2480 Ma, respectively
301 (Fig. 8f).

302 Three samples (grey sandstone), CZ05 (103°24'6"E, 29°37'23"N), CZ01 (103°24'22"E,
303 29°37'20"N), and CZ03 (103°24'43.2"E, 29°37'27"N), were collected from the upper part of the Xujiahe
304 Formation in the Chuanzhu section (Fig. 6). The KDE plots of these samples are similar, showing peaks
305 at ~276 Ma, ~429 Ma, ~1030 Ma, ~1860 Ma and ~2470 Ma (Fig. 8g-i).

306

307 **DISCUSSION**

308 **Detrital sources**

309 *Zircon spectra of potential sources*

310 As suggested by previous detrital zircon studies of the Sichuan Basin (Deng *et al.*, 2008; Weislogel
311 *et al.*, 2010; Chen, 2011; Luo *et al.*, 2014; Zhang *et al.*, 2015; Shao *et al.*, 2016; Zhu *et al.*, 2017), potential
312 source terrains for the Triassic strata include eastern Songpan-Ganzi terrane, northern and southern
313 Kangdian, Longmen Shan thrust belt, Qinling orogen, southeastern Yangtze Block .

314 We compiled zircon U-Pb ages of the crystalline and clastic rocks exposed in these potential source
315 areas (Fig. 9). The detrital zircon U-Pb age spectrum of the eastern Songpan-Ganzi terrane shows three
316 major peaks at ~290Ma, ~430Ma, ~1870Ma, and two minor peaks at ~770Ma, ~950Ma, ~2480Ma (Fig.
317 9f). The northern Kangdian basement is characterised by two major peaks at ~800Ma and ~930Ma, and
318 a minor peak at ~260Ma (Fig. 9g); whereas the southern Kangdian basement is more complex, with
319 peaks at ~810Ma, ~1840Ma, and three minor peaks at ~2310Ma and ~2430Ma (Fig. 9h). The Longmen
320 Shan thrust belt produces three major peaks at ~520Ma, ~750M and, ~945Ma (Fig. 9i). The Qinling
321 orogen is characterised by three major peaks at ~440Ma, ~815Ma and ~1995Ma, and three minor peaks

322 at ~260Ma, ~1830Ma and ~2465Ma (Fig. 9j). The southeastern Yangtze Block yields a dominant peak
323 at ~815Ma (Fig. 9k).

324 It is worth noting that ratios between components of the age spectra of potential source areas may
325 not representative, even though hundreds of single ages have been compiled. This is because the spectra
326 are mostly derived from a collection of few detrital studies of Neoproterozoic sediments, covering little
327 parts of the source area (Figs. 9g, 9i and 9j). For example, the age data of north Kangdian basement are
328 mostly (336 out of 407) derived from the detrital zircon U-Pb age of Neoproterozoic Yanbian Group
329 (Zhou *et al.*, 2006 and Sun *et al.*, 2009), 37 out of 407 dates are crystallization ages of Neoproterozoic
330 igneous rocks, which are of ~800 Ma (Fig. 9g), whereas the rest 34 dates from Upper Permian sandstone
331 samples are of ~260 Ma, which is likely derived from Emeishan igneous province (He *et al.*, 2007).
332 Further, the areas of these rock types and the abundances of zircon therein are significant variable. For
333 these reasons, our data interpretation ignores the proportions of age peaks.

334 *Detrital sources of the Lower and Middle Triassic strata*

335 Detrital zircon age of four Lower and Middle Triassic samples (LCG01, LMD02, LCG03, LCG04.)
336 defines a prominent peak at ~810 Ma. It is worth noting that two of four sample (LCG01, LCG04)
337 exhibits three minor peaks at ~255 Ma, ~535 Ma and ~970 Ma, which are missing from the samples LCG
338 02 and LMD02 (Fig. 8).

339 The ~810 Ma age peak presents in two potential source areas, the northern Kangdian basement and
340 the southeastern Yangtze Block). The most likely source is the northern Kangdian basement. The age
341 spectra of crystalline rocks of the northern Kangdian basement is dominated by the peak at ~800 Ma,
342 similar to that of the Lower and Middle Triassic sediments. However, the bulk age spectra of the northern
343 Kangdian basement also include a major peak at ~930 Ma, which forms a minor component in the Lower
344 and Middle Triassic sediments. This suggests the Neoproterozoic meta-sediments, from which the ~930
345 Ma age peak were derived (Fig. 9g), were not a major source, probably because the exposure of the meta-
346 sediments is relatively limited.

347 Further, detrital zircon age spectra of Lower and Middle Triassic samples include a minor peak at
348 ~535 Ma that has only been recognized in the Longmen Shan (Figs. 9a, i), indicating the Longmen Shan
349 was possibly also a source of sediments. Furthermore, the interpretation in terms of the source area is
350 also consistent with the eastward paleocurrent directions of these Lower and Middle Triassic sediments
351 (Fig. 5).

352 Furthermore, our zircon age compilation for the northern Kangdian basement also shows a minor
353 peak at ~255 Ma, derived from the Emeishan basalt (He *et al.*, 2007). However, this age peak is either
354 minor or absent from the age spectra of the lower and middle Triassic strata. This is probably because of
355 the relatively lower concentration of zircons in mafic rocks.

356 The southeastern Yangtze Block cannot be ruled out as a possible source; but the possibility is very
357 low. If the southeastern Yangtze Block were the source, it would require a long drainage system to deliver
358 the sediments into the southwestern Sichuan Basin via the northern Kangdian, because the southeastern
359 Yangtze Block and the southwestern Sichuan Basin were separated by a N-S striking depocenter, running
360 across the central part of the basin (Fig. 4a), where coeval deposits are composed of carbonate, shale and
361 mudstone (Hu, *et al.*, 2010; Tan, *et al.*, 2014; Sun, *et al.*, 2015).

363 In contrast to the Lower-Middle Triassic samples, detrital zircons from the Upper Triassic samples
364 (LCG05, LCG06, CZ05, CZ01, CZ03), which exhibit southeastward paleocurrent directions (Fig. 5), are
365 characterized by multiple age peaks at ~270 Ma, ~435 Ma, ~775Ma and ~1010 Ma, ~1840Ma and 2480
366 Ma (Fig. 9b). Detrital zircon data of the coeval sediments in the southwestern, western and northern
367 Sichuan Basin, as reported in previous studies, yield similar age spectra (Figs. 9c, d, e), indicating that
368 they may have the same or similar sources, including the Qinling orogen, Longmen Shan thrust belt, and
369 eastern Songpan-Ganzi terrane (Chen, 2011; Luo *et al.*, 2014; Zhang *et al.*, 2015; Shao *et al.*, 2016).

370 Similar age spectra are shown by the Triassic turbidites of the eastern Songpan-Ganzi terrane
371 (Weislogel *et al.*, 2010; Ding *et al.*, 2013; Zhang, 2014), which may have shared similar sources as the
372 Sichuan Basin. Alternatively, the eastern Songpan-Ganzi terrane may have experienced a phase of
373 shortening in response to the late Triassic intracontinental orogeny along the Longmen Shan thrust belt
374 (Li *et al.*, 2003a; Yan *et al.*, 2011; Zheng *et al.*, 2016). From this perspective, it is speculated that the
375 eastern Songpan-Ganzi terrane might also be a source region for the Upper Triassic detritus of the
376 Sichuan Basin.

377 To summarize, the detrital zircon results presented above suggest the source areas for the detritus
378 of the southwestern Sichuan Basin changed significantly from the Northern Kangdian basement to the
379 Qinling orogeny - Longmen Shan thrust belt - eastern Songpan-Ganzi terrane at late Triassic time. Such
380 a change indicates the adjustment of the Triassic sediment route system, which has significant
381 palaeogeographic and tectonic implications.

382

383 **Tectonic and palaeogeographic implications**

384 Despite of the significant change in the detrital zircon spectra, palaeocurrent of the Lower, Middle
385 and Upper Triassic strata has barely changed. They are mostly eastward. This indicate that the Kangdian
386 Basement, which is now south of the study area, was located west (Fig. 10a), indicating that the basement
387 should have experienced considerable eastward displacement relative to the Sichuan Basin. Such an
388 interpretation is consistent with the late Mesozoic and Cenozoic deformation history of the region.
389 Further, as indicated by the migration of the Mesozoic depocenters in the Sichuan Basin, Meng *et al.*
390 (2005) suggest the Basin has experienced considerable clockwise rotation during Mesozoic time. Further,
391 late Cenozoic left-lateral strike-slip along the Xianshuihe fault has displaced the Kangdian basement
392 eastward from the Longmen Shan by ~80 km (Wang *et al.*, 2009; Tian *et al.*, 2014).

393 Upper Triassic sediments in the Sichuan Basin were mainly sourced from the Qinling orogeny and
394 the Longmen Shan thrust belt, as suggested by previous studies (Fig. 9, 10b) (Deng *et al.*, 2008; Chen,
395 2011; Luo *et al.*, 2014; Zhang *et al.*, 2015; Shao *et al.*, 2016; Zhu *et al.*, 2017). The sediment route system
396 is mostly eastward and southeastward, as indicated by the paleocurrent (Fig. 5). The similarity in detrital
397 zircon signal between the upper Triassic sediments and the eastern Songpan-Ganzi terrane indicates that
398 the eastern Songpan-Ganzi terrane might also have been significantly shortened and unroofed, providing
399 detritus for the western and southern Sichuan Basin. The Late Triassic shortening of the Songpan-Ganzi
400 turbidites might relate to several possible processes, including (1) westward subduction of the Ganzi–
401 Litang Ocean during the Late Triassic (Hou *et al.*, 2004), (2) collision between Yidun arc and the
402 Songpan-Ganzi terrane at the end of the Triassic (Hou *et al.*, 2004; Wang *et al.*, 2013b), (3) intra-
403 continental transpressional shortening between the eastern Songpan-Ganzi terrane and the Sichuan Basin,

404 forming the Longmen Shan thrust belt (e.g., Li *et al.*, 2003a; Harrowfield and Wilson, 2005; Wang and
405 Meng, 2008), and (4) slab retreat or rollback of Paleo-Tethys lithosphere (e.g., de Sigoyer *et al.*, 2014;
406 Pullen *et al.*, 2008; Zhang *et al.*, 2015).

407 Late Triassic uplift and unroofing of the Longmen Shan thrust belt is required to provide detritus
408 for the Upper Triassic deposits, as discussed above. This speculation is consistent with other lines of
409 evidence. First, the presence of klippen of Paleozoic and Precambrian rocks over Triassic sediments in
410 the eastern front of the Longmen Shan thrust belt indicate that these structures were formed during the
411 Late Triassic or later. Second, the oldest U–Th–Pb monazite and Sm–Nd garnet ages (204–190 Ma),
412 derived from metamorphosed rocks in the Danba Antiform, immediately south of the Longmen Shan
413 thrust belt, were interpreted as dating the timing of Barrovian metamorphism associated with the
414 deformation (Huang *et al.*, 2003; Weller *et al.*, 2013). Third, muscovite $^{40}\text{Ar}/^{39}\text{Ar}$ dating of early
415 Paleozoic schist and Neoproterozoic Pengguan complex from the northern and middle Longmen Shan
416 yielded ages between 237–208 Ma and 235–226 Ma, respectively, which were interpreted as minimum
417 age constraints for Mesozoic crustal shortening (Yan *et al.*, 2011; Zheng *et al.*, 2016).

418 As indicated by our palaeocurrent and detrital zircon results, the northern Kangdian basement was
419 uplifted and unroofed to provide the detritus for the Lower and Middle Triassic sediments in the
420 southwestern Sichuan Basin (Fig. 10a). However, in late Triassic time, the basement subsided
421 significantly in Late Triassic time (Fig. 10b), as indicated by the presence of Upper Triassic sediments
422 (~1 km, Guo *et al.*, 1996) over the basement rocks (Fig. 2). The subsidence of the basement might result
423 from the eastward shortening and loading of the Songpan-Ganze terrane over the western margin of the
424 Yangtze Block in response to the Late Triassic collision between Yangtze Block, Yidun arc and
425 Qiangtang Terrane along the Ganzi-Litang and Jinshajiang sutures (Fig. 10b). This interpretation is also
426 supported by the eastward paleocurrent and the development of a ~1.5-km-thick late Triassic depocenter
427 in areas south of the sampling sites (i.e. the location of the northern Kangdian basement) (Fig. 4c). Such
428 a tectonic reconstruction differs from previous models, suggesting continuous Late Permian to Jurassic
429 subsiding as a rift (Luo, 1983; Guo *et al.*, 1996), or early Mesozoic transtensional subsidence by strike-
430 slip faulting (Chen *et al.*, 1987; Feng *et al.*, 1994; Wang *et al.*, 1994; He *et al.*, 2003; Chen *et al.*, 2011).
431

432 CONCLUSIONS

433 Triassic sediments in the southwestern Sichuan Basin record different detrital zircon geochronology
434 signals. Detrital zircon age spectra of Lower and Middle Triassic samples are similar and characterized
435 by a dominant age mode at ~810 Ma, with three minor peaks at ~255Ma, ~535Ma and ~970Ma. In
436 contrast to the Lower-Middle Triassic samples, detrital zircon spectra of Upper Triassic samples are
437 characterized by multiple age peaks at ~270 Ma, ~435 Ma, ~775Ma and ~1010 Ma, ~1840Ma and ~2480
438 Ma.

439 Our data reveal a major change of provenance during the Upper Triassic in response to multiple
440 tectonic events. The sediments in the southwestern Sichuan Basin is supplied by the highland of the
441 Yangtze Block (the northern Kangdian Basement) during the Early-Middle Triassic passive continental
442 margin stage. During the Upper Triassic, the Sichuan Basin was inverted into a foreland basin and the
443 Longmen Shan thrust belt and possibly the eastern Songpan-Ganzi terrane was uplifted in response to
444 the closure of the Paleo-Tethys Ocean and intra-continental shortening along the Longmen Shan thrust
445 belt, becoming the main source areas of the southwestern and western Sichuan Basin. The Late Triassic

446 sediments in the southwestern Sichuan Basin have recorded the collision and subsequent continuing
447 convergence between Qiangtang Block and Yangtze Block. This study highlights the importance of
448 tectonic events in reorganizing drainage and sediment supply in foreland basins. The Late Triassic
449 evolution of foreland basin in the Upper Yangtze Block Sichuan Basin have been strongly controlled by
450 collision and subsequent continuing convergence between Qiangtang Terrane and Yangtze Block,
451 challenging the previous view that the foreland basin was mainly controlled by the collision between
452 northern China Block and Yangtze Block.

453

454

455 **ACKNOWLEDGEMENTS**

456 We thank Yan Liang, Yun Kun, Chen Bin, Wang Weiming, Lu Yanqi and Zhou Qiwei for their help
457 in the field. This work benefited from discussions with Profs. Hu Xiumian, Dr. Dong Shunli and Dr.
458 Chen Yang. Funding for this research was provided by National Natural Science Foundation of China
459 (Grant No. 41502116, 41772211, 41372114 and 41340005), Chinese 1000 Young Talents Program and
460 the National Key Laboratory of Oil and Gas Reservoir Geology and Exploitation (Grant No. PLC201604).
461 Constructive reviews by Drs. Amy Weislogel, Alex Pullen, an anonymous reviewer, and the editor Dr.
462 Nadine McQuarrie clarified many points in this article.

463 **REFERENCES**

- 464 ALI, J.R., FITTON, J.G. & HERZBERG, C. (2010) Emeishan large igneous province (SW China) and the
465 mantle-plume up-doming hypothesis. *Journal of the Geological Society*, **167**, 953-959.
- 466 ALI, J.R., THOMPSON, G.M., SONG, X. & WANG, Y. (2002) Emeishan Basalts (SW China) and the 'end-
467 Guadalupian' crisis: magnetobiostratigraphic constraints. *Journal of the Geological Society*, **159**,
468 21-29.
- 469 BGMRS (Bureau of Geology and Mineral Resources, Sichuan Province), 1991. Regional Geology of
470 Sichuan Province. Geological Publishing House, Beijing, in Chinese.
- 471 BGMRS (Bureau of Geology and Mineral Resources, Sichuan Province), 1997. Multiple stratigraphic
472 division research in China: lithostratigraphy in Sichuan Province. China University of Geosciences
473 Press, Wuhan, 1-417 pp, in Chinese.
- 474 BGSP (Bureau of Geology, Sichuan Province), 1974. Bureau of Geology and Mineral Resources of
475 Sichuan Province. Regional Geological Report of Yingjing Sheet (1:200000). Geological
476 Publishing House, Beijing, 1-143 pp, in Chinese.
- 477 BURCHFIELD, B.C., CHEN, Z., LIU, Y. & ROYDEN, L.H. (1995) Tectonics of the Longmen Shan and
478 adjacent regions, central China. *International Geology Review*, **37**, 661-735.
- 479 BUREAU OF GEOLOGY AND MINERAL RESOURCES, S.P.B. (1997). *Multiple stratigraphic division*
480 *research in China: lithostratigraphy in Sichuan Province*. China University of Geosciences Press,
481 Wuhan, 1-143 pp, in Chinese.
- 482 BURGESS, S.D., BOWRING, S.A. & SHEN, S. (2014) High-precision timeline for Earth's most severe
483 extinction. *Proceedings of the National Academy of Sciences of the United States of America*, **111**,
484 3316-3321.
- 485 CHANG, E.Z. (2000) Geology and Tectonics of the Songpan-Ganzi Fold Belt, Southwestern China.
- 486 CHEN, Q., SUN, M., LONG, X., ZHAO, G. & YUAN, C. (2016) U - Pb ages and Hf isotopic record of zircons
487 from the late Neoproterozoic and Silurian - Devonian sedimentary rocks of the western Yangtze
488 Block: Implications for its tectonic evolution and continental affinity. *Gondwana Research*.
- 489 CHEN, Y. (2011) The Formation of Western Sichuan Foreland Basin and Its Significance in Oil-gas
490 Exploration During Late Triassic, Chengdu University of Technology, Chengdu, 1-170 pp, in
491 Chinese with English abstract.
- 492 DAI, S., REN, D., CHOU, C., FINKELMAN, R.B., SEREDIN, V.V. & ZHOU, Y. (2012) Geochemistry of trace
493 elements in Chinese coals: A review of abundances, genetic types, impacts on human health, and

- 494 industrial utilization. *International Journal of Coal Geology*, **94**, 3-21.
- 495 DE SIGOYER, J., VANDERHAEGHE, O., DUCHÊNE, S. & BILLEROT, A. (2014) Generation and emplacement
496 of Triassic granitoids within the Songpan Ganze accretionary-orogenic wedge in a context of slab
497 retreat accommodated by tear faulting, Eastern Tibetan plateau, China. *Journal of Asian Earth
498 Sciences*, **88**, 192-216.
- 499 DECELLES, P.G., LANGFORD, R.P. & SCHWARTZ R. K. (1983) Two new methods of paleocurrent
500 determination from trough cross-stratification. *Journal of Sedimentary Research*, **53**: 629-642
- 501 DENG, F., JIA, D., LUO, L., LI, H., LI, Y. & WU, L. (2008) The contrast between provenances of Songpan-
502 Ganze and Western Sichuan foreland basin in the Late Triassic: clues to the tectonics and
503 palaeogeography. *Geological Review*, **54**, 561-573, in Chinese with English abstract.
- 504 DENG, K., HE, L., QIN, D. & HE, Z. (1982) The earlier Late Triassic sequence and its sedimentary
505 environment in western Sichuan Basin. *Oil & Gas Geology*, **3**, 204-210, in Chinese with English
506 abstract.
- 507 DING, L., YANG, D., CAI, F.L., PULLEN, A., KAPP, P., GEHRELS, G.E., ZHANG, L.Y., ZHANG, Q.H., LAI,
508 Q.Z., YUE, Y.H. & SHI, R.D. (2013) Provenance analysis of the Mesozoic Hoh-Xil-Songpan-Ganzi
509 turbidites in northern Tibet: Implications for the tectonic evolution of the eastern Paleo-Tethys
510 Ocean. *Tectonics*, **32**, 34-48.
- 511 DUAN, L., MENG, Q., ZHANG, C. & LIU, X. (2011) Tracing the position of the South China block in
512 Gondwana: U - Pb ages and Hf isotopes of Devonian detrital zircons. *Gondwana Research*, **19**,
513 141-149.
- 514 ENKELMANN, E., WEISLOGEL, A., RATSCHBACHER, L., EIDE, E., RENNO, A. & WOODEN, J. (2007) How
515 was the Triassic Songpan-Ganzi basin filled? A provenance study. *Tectonics*, **26**, n/a-n/a.
- 516 FENG, Z., BAO, Z. & LI, S. (1997) Potential of oil and gas of the Middle and Lower Triassic of south
517 China from the viewpoint of lithofacies paleogeography. *Journal of the University of Petroleum ,
518 China*, **21**, 1-6, in Chinese with English abstract.
- 519 FENG, Z., JIN, Z., HE, Y., BAO, Z. & XIN, W. (1994) *Lithofacies paleogeography of Permian of Yunnan-
520 Guizhou-Guangxi Region*. Geological Publishing House, Beijing, 1-146 pp, in Chinese with English
521 abstract.
- 522 FU, B., KITA, N.T., WILDE, S.A., LIU, X., CLIFF, J. & GREIG, A. (2013) Origin of the Tongbai-Dabie-
523 Sulu Neoproterozoic low- δ 18O igneous province, east-central China. *Contributions to Mineralogy
524 and Petrology*, **165**, 641-662.
- 525 GENG, Y., YANG, C., WANG, X. & LIUDONG, R. (2007) Age of Crystalline basement in Western Margin
526 of Yangtze Terrane. *Geological Journal of China Universities*, **13**, 429-441, in Chinese with English
527 abstract.
- 528 GRADSTEIN, F.M., OGG, J.G., SCHMITZ, M. & OGG, G. (2012) The Geologic Time Scale 2012 2-Volume
529 Set.
- 530 GRIFFIN, W.L., POWELL, W.J., PEARSON, N.J., O'REILLY, S.Y. & A, E.M. (2008) GLITTER: data
531 reduction software for laser ablation ICP-MS. In: *Laser Ablation-ICP-MS in the earth sciences* (Ed.
532 by P. S. ED.), **40**, 204-207. Mineralogical association of Canada short course series.
- 533 GUO, J., YOU, Z., YANG, J., SHEN, W., XU, S. & WANG, R. (1998) Studying on the U-Pb dating of zircon
534 in Tianwan and Pianlugang bodies from Shimian area, west Sichuan. *Journal of Mineralogy and
535 Petrology*, **18**, 92-95, in Chinese with English abstract.
- 536 GUO, Z., DENG, K., HAN, Y. & LIU, Y. (1996) *The Formation and Development of Sichuan Basin*.
537 Geological Publishing House, Beijing, 1-200 pp, in Chinese with English abstract.
- 538 HARROWFIELD, M.J. & WILSON, C.J.L. (2005) Indosinian deformation of the Songpan Garzê Fold Belt,
539 northeast Tibetan Plateau. *Journal of Structural Geology*, **27**, 101-117. HE, B., XU, Y., GUAN, J. &
540 ZHONG, Y. (2010) Paleokarst on the top of the Maokou Formation: Further evidence for domal
541 crustal uplift prior to the Emeishan flood volcanism. *Lithos*, **119**, 1-9.
- 542 HE, B., XU, Y., HUANG, X., LUO, Z., SHI, Y., YANG, Q. & YU, S. (2007) Age and duration of the Emeishan
543 flood volcanism, SW China: Geochemistry and SHRIMP zircon U - Pb dating of silicic ignimbrites,
544 post-volcanic Xuanwei Formation and clay tuff at the Chaotian section. *Earth and Planetary
545 Science Letters*, **255**, 306-323.
- 546 HE, B., XU, Y., XIAO, L. & WANG, Y. (2003) Does the Panzhihua-Xichang Rift Exist? *Geological Review*,
547 **49**, 572-582, in Chinese with English abstract.
- 548 HOU, Z., YANG, Y., QU, X., HUANG, D., LU, Q., WANG, H., YU, J. & TANG, S. (2004) Tectonic evolution
549 and mineralization systems of the Yidun Arc orogen in Sanjiang region, China. *Acta Geologica
550 Sinica*, **78**, 109-120, in Chinese with English abstract.
- 551 HU, M., WEI, G., LI, S., YANG, W., ZHU, L. & YANG, Y. (2010) Characteristics of Sequence-based
552 Lithofacies and Paleogeography, and Reservoir Prediction of the Jialingjiang Formation in Sichuan
553 Basin. *Acta Sedimentologica Sinica*, **28**, 1145-1152, in Chinese with English abstract.

- 554 HUANG, H., CAWOOD, P.A., HOU, M., YANG, J., NI, S., DU, Y., YAN, Z. & WANG, J. (2016) Silicic ash
555 beds bracket Emeishan Large Igneous province to <1m.y. at ~260Ma. *Lithos*, **264**, 17-27.
- 556 HUANG, M., BUICK, I.S. & HOU, L.W. (2003) Tectonometamorphic Evolution of the Eastern Tibet
557 Plateau: Evidence from the Central Songpan - Garzê Orogenic Belt, Western China. *Journal of*
558 *Petrology*, **44**, 255-278.
- 559 HUANG, S., HUANG, K., ZHONG, Y., LI, X., MAO, X., HU, Z., LIU, S., ZHANG, M. & WU, W. (2017)
560 Carbon isotope composition and comparison of Lower Triassic marine carbonate rocks from
561 Southern Longmenxia section in Guang'an, Sichuan Basin. *Science China Earth Sciences*, 57-71,
562 in Chinese with English abstract.
- 563 HUANG, X., XU, Y., LAN, J., YANG, Q. & LUO, Z. (2009) Neoproterozoic adakitic rocks from Mopanshan
564 in the western Yangtze Craton: Partial melts of a thickened lower crust. *Lithos*, **112**, 367-381.
- 565 JACKSON, S.E., PEARSON, N.J., GRIFFIN, W.L. & BELOUSOVA, E.A. (2004) The application of laser
566 ablation-inductively coupled plasma-mass spectrometry to in situ U - Pb zircon geochronology.
567 *Chemical Geology*, **211**, 47-69.
- 568 JIA, D., WEI, G., CHEN, Z., LI, B., ZENG, Q. & YANG, G. (2006) Longmen Shan fold-thrust belt and its
569 relation to the western Sichuan Basin in central China: New insights from hydrocarbon exploration.
570 *Bulletin*, **90**, 1425-1447.
- 571 JIANG, Z., TIAN, J., CHEN, G., LI, X. & ZHANG, M. (2007) Sedimentary characteristics of the Upper
572 Triassic in western Sichuan foreland basin. *Journal of Palaeogeography*, **9**, 143-154, in Chinese
573 with English abstract.
- 574 JOCHUM, K.P., WEIS, U., STOLL, B., KUZMIN, D., YANG, Q., RACZEK, I., JACOB, D.E., STRACKE, A.,
575 BIRBAUM, K., FRICK, D.A., GÜNTHER, D. & ENZWEILER, J. (2011) Determination of Reference
576 Values for NIST SRM 610-617 Glasses Following ISO Guidelines. *Geostandards and*
577 *Geoanalytical Research*, **35**, 397-429.
- 578 LEHRMANN, D.J., STEPCHINSKI, L., ALTINER, D., ORCHARD, M.J., MONTGOMERY, P., ENOS, P.,
579 ELLWOOD, B.B., BOWRING, S.A., RAMEZANI, J. & WANG, H. (2015) An integrated biostratigraphy
580 (conodonts and foraminifers) and chronostratigraphy (paleomagnetic reversals, magnetic
581 susceptibility, elemental chemistry, carbon isotopes and geochronology) for the Permian - Upper
582 Triassic strata of Guandao section, Nanpanjiang Basin, south China. *Journal of Asian Earth*
583 *Sciences*, **108**, 117-135.
- 584 LI, C. (1963) A preliminary study of the tectonic development of the "Kang-Dian Axis". *Acta Geologica*
585 *Sinica*, **43**, 214-229, in Chinese with English abstract.
- 586 LI, X., LI, Z., ZHOU, H., LIU, Y. & KINNY, P.D. (2002) U - Pb zircon geochronology, geochemistry and
587 Nd isotopic study of Neoproterozoic bimodal volcanic rocks in the Kangdian Rift of South China:
588 implications for the initial rifting of Rodinia. *Precambrian Research*, **113**, 135-154.
- 589 LI, X., ZHOU, H., LI, Z., LIU, Y. & P., K. (2001) Zircon U-Pb age and petrochemical characteristics of
590 the Neoproterozoic bimodal volcanics from western Yangtze block. *Geochimica*, **30**, 315-322, in
591 Chinese with English abstract.
- 592 LI, Y., ALLEN, P.A., DENSMORE, A.L. & QIANG, X. (2003a) Evolution of the Longmen Shan foreland
593 basin (western Sichuan, China) during the Late Triassic Indosinian orogeny. *Basin Research*, **15**,
594 117-138.
- 595 LI, Y., HE, D., LI, D., WEN, Z., MEI, Q., LI, C. & SUN, Y. (2016) Detrital zircon U-Pb geochronology
596 and provenance of Lower Cretaceous sediments: Constraints for the northwestern Sichuan pro-
597 foreland basin. *Palaeogeography, Palaeoclimatology, Palaeoecology*, **453**, 52-72.
- 598 LI, Y., SHAO, L., ERIKSSON, K.A., TONG, X., GAO, C. & CHEN, Z. (2014) Linked sequence stratigraphy
599 and tectonics in the Sichuan continental foreland basin, Upper Triassic Xujiahe Formation,
600 southwest China. *Journal of Asian Earth Sciences*, **88**, 116-136.
- 601 LI, Y., YAN, Z., LIU, S., LI, H., CAO, J., SU, D., DONG, S., SUN, W., YANG, R. & YAN, L. (2014) Migration
602 of the carbonate ramp and sponge buildup driven by the orogenic wedge advance in the early stage
603 (Carnian) of the Longmen Shan foreland basin, China. *Tectonophysics*, **619-620**, 179-193.
- 604 LI, Z.X., LI, X.H., KINNY, P.D., WANG, J., ZHANG, S. & ZHOU, H. (2003b) Geochronology of
605 Neoproterozoic syn-rift magmatism in the Yangtze Craton, South China and correlations with other
606 continents: evidence for a mantle superplume that broke up Rodinia. *Precambrian Research*, **122**,
607 85-109.
- 608 LIN, G. (2010) Zircon U-Pb age and petrochemical characteristics of Shimian granite in western Sichuan:
609 petrogenesis and tectonic significance. *Earth Science-Journal of China University of Geoscience*,
610 **35**, 611-620, in Chinese with English abstract.
- 611 LIN, G., LI, X. & LI, W. (2006b) SHRIMP U-Pb zircon age, geochemistry and Nd-Hf isotope of
612 Neoproterozoic mafic dyke swarms in western Sichuan: Petrogenesis and tectonic significance.
613 *SCIENCE CHINA: Earth Sciences*, **36**, 630-645, in Chinese with English abstract.

- 614 LIN, L., CHEN, H., ZHAI, C., XIAOQIANG, H. & JUNWEN, L. (2006a) Sandstone compositions and
615 paleogeographic evolution of the Upper Triassic Xujiahe formation in the western Sichuan basin,
616 China. *Petroleum Geology and Experiment*, **28**, 511-517, in Chinese with English abstract.
- 617 LIN, W., WANG, H. & SONG, H. (1982) Upper Permian to Lower-middle Triassic Strata and Sedimentary
618 Environments in Longmendong, Emei, Sichuan. *Journal of Mineralogy and Petrology*, 53-58.
- 619 LIU, Z. & TONG, J. (2001) The Middle Triassic Stratigraphy and Sedimentary Paleogeography of South
620 China. *Acta Sedimentologica Sinica*, **19**, 327-332, in Chinese with English abstract.
- 621 LONG, S., WU, S., LI, H., BAI, Z., MA, J. & ZHANG, H. (2011) Hybrid sedimentation in Late Permian-
622 Early Triassic in western Sichuan basin, China. *J. Earth Sci.*, **22**, 340-350.
- 623 LUO, L., QI, J., ZHANG, M., WANG, K. & HAN, Y. (2014) Detrital zircon U - Pb ages of Late Triassic -
624 Late Jurassic deposits in the western and northern Sichuan Basin margin: constraints on the foreland
625 basin provenance and tectonic implications. *Int J Earth Sci (Geol Rundsch)*, **103**, 1553-1568.
- 626 LUO, Y. (1983) The evolution of paleoplates in the Kang-Dian tectonic zone. *Earth Science-Journal of*
627 *Wuhan College of Geology*, **22**, 93-102, in Chinese with English abstract.
- 628 LUO, Z., SUN, W., HAN, J. & WANG, R. (2012) Effect of Emei mantle plume on the conditions of Permian
629 accumulation in middle-upper Yangtze area. *Earth Science Frontiers*, **19**, 144-154, in Chinese with
630 English abstract.
- 631 MENG, E., LIU, F., DU, L., LIU, P. & LIU, J. (2015) Petrogenesis and tectonic significance of the Baoxing
632 granitic and mafic intrusions, southwestern China: Evidence from zircon U - Pb dating and Lu -
633 Hf isotopes, and whole-rock geochemistry. *Gondwana Research*, **28**, 800-815.
- 634 MENG, Q. & ZHANG, G. (2000) Geologic framework and tectonic evolution of the Qinling orogen, central
635 China. *Tectonophysics*, **323**, 183-196.
- 636 MENG, Q., WANG, E. & HU, J. (2005) Mesozoic sedimentary evolution of the northwest Sichuan basin:
637 Implication for continued clockwise rotation of the South China block. *Geol Soc America Bull*, **117**,
638 396.
- 639 OVTCHAROVA, M., BUCHER, H., SCHALTEGGER, U., GALFETTI, T., BRAYARD, A. & GUEX, J. (2006) New
640 Early to Middle Triassic U - Pb ages from South China: Calibration with ammonoid
641 biochronozones and implications for the timing of the Triassic biotic recovery. *Earth and Planetary*
642 *Science Letters*, **243**, 463-475.
- 643 PULLEN, A., KAPP, P., GEHRELS, G.E., VERVOORT, J.D. & DING, L. (2008) Triassic continental
644 subduction in central Tibet and Mediterranean-style closure of the Paleo-Tethys Ocean. *Geol*, **36**,
645 351.
- 646 REID, A.J., WILSON, C.J.L. & LIU, S. (2005) Structural evidence for the Permo-Triassic tectonic evolution
647 of the Yidun Arc, eastern Tibetan Plateau. *Journal of Structural Geology*, **27**, 119-137.
- 648 ROGER, F. & CALASSOU, S. (1997) Géochronologie U-Pb sur zircons et géochimie (Pb, Sr et Nd) du socle
649 de la chaîne de Songpan-Garze (Chine). *Comptes Rendus de l'Académie des Sciences-Series IIA-*
650 *Earth and Planetary Science*, **324**, 819-826.
- 651 ROGER, F., JOLIVET, M., CATTIN, R. & MALAVIEILLE, J. (2011) Mesozoic-Cenozoic tectonothermal
652 evolution of the eastern part of the Tibetan Plateau (Songpan-Garze, Longmen Shan area): insights
653 from thermochronological data and simple thermal modelling. *Geological Society, London, Special*
654 *Publications*, **353**, 9-25.
- 655 ROGER, F., JOLIVET, M. & MALAVIEILLE, J. (2008) Tectonic evolution of the Triassic fold belts of Tibet.
656 *Comptes Rendus Geoscience*, **340**, 180-189.
- 657 RUAN, L. (2013) The Metallogenic Regularity of Dashuigou Tellurium Deposit, Shimian, Sichuan
658 Province and the Origination of Prospecting, China University of Geosciences, Wuhan, in Chinese
659 with English abstract.
- 660 SHAO, T., CHENG, N. & SONG, M. (2016a) Provenance and tectonic-paleogeographic evolution:
661 Constraints from detrital zircon U - Pb ages of Late Triassic-Early Jurassic deposits in the northern
662 Sichuan basin, central China. *Journal of Asian Earth Sciences*, **127**, 12-31.
- 663 SHAO, T., CHENG, N. & SONG, M. (2016b) Provenance and tectonic-paleogeographic evolution:
664 Constraints from detrital zircon U - Pb ages of Late Triassic-Early Jurassic deposits in the northern
665 Sichuan basin, central China. *Journal of Asian Earth Sciences*, **127**, 12-31.
- 666 SHEN, W., GAO, J., XU, S., LI, H., ZHOU, G., YANG, Z. & YANG, Q. (2003) Geochemical Characteristics
667 of the Shimian Ophiolite, Sichuan Province and Its Tectonic Significance. *Geological Review*, **49**,
668 17-27, in Chinese with English abstract.
- 669 SHEN, W., LI, H., XU, S. & WANG, R. (2000) U-Pb Chronological Study of Zircons from the
670 Huangcaoshan and Xiasuozi Granites in the Western Margin of Yangtze Plate. *Geological Journal*
671 *of China Universities*, **6**, 412-416, in Chinese with English abstract.
- 672 SHI, Z., PRETO, N., JIANG, H., KRYSSTYN, L., ZHANG, Y., OGG, J.G., JIN, X., YUAN, J., YANG, X. & DU,
673 Y. (2016) Demise of Late Triassic sponge mounds along the northwestern margin of the Yangtze

- 674 Block, South China: Related to the Carnian Pluvial Phase? *Palaeogeography Palaeoclimatology*
675 *Palaeoecology*.
- 676 SHI, Z., WANG, Z., HAO, C., GUO, Z. & MO, W. (2015) Sedimentary Facies of the Upper Triassic
677 Maantang Formation in Sichuan Basin. *Journal of Palaeogeography*, **17**, 771-786, in Chinese with
678 English abstract.
- 679 SHI, Z., YANG, W., XIE, Z., JIN, H. & XIE, W. (2010) Upper Triassic Clastic Composition in Sichuan
680 Basin, Southwest China: Implication for Provenance Analysis and the Indosinian Orogeny. *ACTA*
681 *GEOLOGICA SINICA*, **84**, 387-397, in Chinese with English abstract.
- 682 SLÁMA, J., KOŠLER, J., CONDON, D.J., CROWLEY, J.L., GERDES, A., HANCHAR, J.M., HORSTWOOD,
683 M.S.A., MORRIS, G.A., NASDALA, L., NORBERG, N., SCHALTEGGER, U., SCHOENE, B., TUBRETT,
684 M.N. & WHITEHOUSE, M.J. (2008) Plešovice zircon — A new natural reference material for U -
685 Pb and Hf isotopic microanalysis. *Chemical Geology*, **249**, 1-35.
- 686 SUN, C., HU, M., HU, Z., XUE, D. & WANG, Z. (2015) Sequence-based Lithofacies and Paleogeography
687 of Lower Triassic Feixianguan Formation in Sichuan Basin. *Marine Origin Petroleum Geology*, 1-
688 9, in Chinese with English abstract.
- 689 SUN, W., ZHOU, M., GAO, J., YANG, Y., ZHAO, X. & ZHAO, J. (2009) Detrital zircon U - Pb
690 geochronological and Lu - Hf isotopic constraints on the Precambrian magmatic and crustal
691 evolution of the western Yangtze Block, SW China. *Precambrian Research*, **172**, 99-126.
- 692 TAN, X., LI, L., LIU, H., CAO, J., WU, X., ZHOU, S. & SHI, X. (2014) Mega-shoaling in carbonate platform
693 of the Middle Triassic Leikoupo Formation, Sichuan Basin, southwest China. *Sci. China Earth Sci.*,
694 **57**, 465-479.
- 695 TAN, X., XIA, Q., CHEN, J., LI, L., LIU, H., LUO, B., XIA, J. & YANG, J. (2013) Basin-scale sand deposition
696 in the Upper Triassic Xujiahe formation of the Sichuan Basin, Southwest China: Sedimentary
697 framework and conceptual model. *Journal of Earth Science*, **24**, 89-103.
- 698 TIAN, Y., KOHN, B.P., GLEADOW, A.J.W. & HU, S. (2013) Constructing the Longmen Shan eastern
699 Tibetan Plateau margin: Insights from low-temperature thermochronology. *Tectonics*, **32**, 576-592.
- 700 TIAN, Y., KOHN, B.P., PHILLIPS, D., HU, S., GLEADOW, A.J.W. & CARTER, A. (2016) Late Cretaceous-
701 earliest Paleogene deformation in the Longmen Shan fold-and-thrust belt, eastern Tibetan Plateau
702 margin: Pre-Cenozoic thickened crust? *Tectonics*, **35**, 2293-2312.
- 703 TIAN, Y., KOHN, B.P., ZHU, C., XU, M., HU, S. & GLEADOW, A.J.W. (2012) Post-orogenic evolution of
704 the Mesozoic Micang Shan Foreland Basin system, central China. *Basin Research*, **24**, 70-90.
- 705 Tian, Y., Kohn, B.P., Gleadow, A.J.W., Hu, S., 2014. A thermochronological perspective on the
706 morphotectonic evolution of the southeastern Tibetan Plateau. *JGR* 119, 676-698.
- 707 XU, Y., HE, B., CHUNG, S., MENZIES, M.A. & FREY, F.A. (2004) Geologic, geochemical, and geophysical
708 consequences of plume involvement in the Emeishan flood-basalt province. *Geology*, **32**, 917.
- 709 VERMEESCH, P. (2012) On the visualisation of detrital age distributions. *Chemical Geology*, **312-313**,
710 190-194.
- 711 WANG, B., WANG, W., CHEN, W.T., GAO, J., ZHAO, X., YAN, D. & ZHOU, M. (2013b) Constraints of
712 detrital zircon U - Pb ages and Hf isotopes on the provenance of the Triassic Yidun Group and
713 tectonic evolution of the Yidun Terrane, Eastern Tibet. *Sedimentary Geology*, **289**, 74-98.
- 714 WANG, B., ZHOU, M., LI, J. & YAN, D. (2011) Late Triassic porphyritic intrusions and associated volcanic
715 rocks from the Shangri-La region, Yidun terrane, Eastern Tibetan Plateau: adakitic magmatism and
716 porphyry copper mineralization. *Lithos*, **127**, 24-38.
- 717 WANG, E. & MENG, Q. (2008) Mesozoic and Cenozoic tectonic evolution of the Longmen Shan fault
718 belt. *Science in CHINA (Series D)*, **38**, 1221-1233. WANG, H., YANG, S. & LI, S. (1983) Mesozoic
719 and Cenozoic basin formation in east China and adjacent regions and development of the continental
720 margin. *Acta Geologica Sinica*, 213-223, in Chinese with English abstract.
- 721 WANG, L. & PAN, G. (2013) *Geological Map of the Qinghai-Tibet plateau and adjacent areas*. Geological
722 Publishing House, Beijing, in Chinese.
- 723 WANG, L., GRIFFIN, W.L., YU, J. & O'REILLY, S.Y. (2010) Precambrian crustal evolution of the Yangtze
724 Block tracked by detrital zircons from Neoproterozoic sedimentary rocks. *Precambrian Research*,
725 **177**, 131-144.
- 726 WANG, L., GRIFFIN, W.L., YU, J. & O'REILLY, S.Y. (2013a) U - Pb and Lu - Hf isotopes in detrital zircon
727 from Neoproterozoic sedimentary rocks in the northern Yangtze Block: implications for
728 Precambrian crustal evolution. *Gondwana Research*, **23**, 1261-1272.
- 729 WANG, L., LU, Y., ZHAO, S. & LUO, J. (1994) *Permian Lithofacies, Paleogeography and Mineralization*
730 *in South China*. Geological Publishing House, Beijing, 1-156pp, in Chinese with English abstract.
- 731 WANG, L., YU, J., GRIFFIN, W.L. & O'REILLY, S.Y. (2012) Early crustal evolution in the western Yangtze
732 Block: evidence from U - Pb and Lu - Hf isotopes on detrital zircons from sedimentary rocks.

- 733 *Precambrian Research*, **222**, 368-385.
- 734 Wang, S., Fang, X., Zheng, D., Wang, E., 2009. Initiation of slip along the Xianshuihe fault zone, eastern
735 Tibet, constrained by K/Ar and fission-track ages. *Int. Geol. Rev.*, 1–11.
- 736 WANG, W. & CENG, C. (1982) The characteristics of alluvial facies of the Lower Triassic Feixianguan
737 formation in the Longmendong, Emei, Sichuan. *Journal of Mineralogy and Petrology*, 71-82, in
738 Chinese with English abstract.
- 739 WANG, W. & ZHOU, M. (2012) Sedimentary records of the Yangtze Block (South China) and their
740 correlation with equivalent Neoproterozoic sequences on adjacent continents. *Sedimentary Geology*,
741 **265-266**, 126-142.
- 742 WANG, Y., ZHANG, Y., FAN, W. & PENG, T. (2005) Structural signatures and 40 Ar/ 39 Ar geochronology
743 of the Indosinian Xuefengshan tectonic belt, South China Block. *Journal of Structural Geology*, **27**,
744 985-998.
- 745 WEI, Y., ZHANG, Z., HE, W., WU, N. & YANG, B. (2014) Evolution of Sedimentary Basins in the Upper
746 Yangtze during Mesozoic. *Editorial Committee of Earth Science-Journal of China University of*
747 *Geosciences*, 1065-1078 in Chinese with English abstract.
- 748 WEISLOGEL, A.L. (2008) Tectonostratigraphic and geochronologic constraints on evolution of the
749 northeast Paleotethys from the Songpan-Ganzi complex, central China. *Tectonophysics*, **451**, 331-
750 345.
- 751 WEISLOGEL, A.L., GRAHAM, S.A., CHANG, E.Z., WOODEN, J.L. & GEHRELS, G.E. (2010) Detrital zircon
752 provenance from three turbidite depocenters of the Middle-Upper Triassic Songpan-Ganzi complex,
753 central China: Record of collisional tectonics, erosional exhumation, and sediment production.
754 *Geological Society of America Bulletin*, **122**, 2041-2062.
- 755 WELLER, O.M., STONGE, M.R., WATERS, D.J., RAYNER, N., SEARLE, M.P., CHUNG, S.L., PALIN, R.M.,
756 LEE, Y. & XU, X. (2013) Quantifying Barrovian metamorphism in the Danba Structural Culmination
757 of eastern Tibet. *Journal of Metamorphic Geology*, **31**, 909-935.
- 758 WGCMSPIB (Write Group of Contiental Mesozoic Stratigraphy and Paleontology in Sichuan Basin of
759 China) (1984) *Contiental Mesozoic Stratigraphy and Paleontology in Sichuan Basin of China*.
760 People's Publishing House of Sichuan, Chengdu.
- 761 WIEDENBECK, M., HANCHAR, J.M., PECK, W.H., SYLVESTER, P., VALLEY, J., WHITEHOUSE, M., KRONZ,
762 A., MORISHITA, Y., NASDALA, L., FIEBIG, J., FRANCHI, I., GIRARD, J.P., GREENWOOD, R.C., HINTON,
763 R., KITA, N., MASON, P.R.D., NORMAN, M., OGASAWARA, M., PICCOLI, P.M., RHEDE, D., SATOH,
764 H., SCHULZ DOBRICK, B., SK R, O., SPICUZZA, M.J., TERADA, K., TINDLE, A., TOGASHI, S.,
765 VENNEMANN, T., XIE, Q. & ZHENG, Y.F. (2004) Further Characterisation of the 91500 Zircon
766 Crystal., **28**, 9-39.
- 767 XIE, J., LI, G. & TANG, D. (2006) Aanlysis on provenance-supply system of Upper Triassic Xujiahe
768 formation, Sichuan Basin. *Natural Gas Exploration and Development*, **29**, 1-3, 13, in Chinese with
769 English abstract.
- 770 XIE, T., ZHOU, Z., ZHANG, Q., HU, S., HUANG, J., WEN, W. & CONG, F. (2013) Zircon U-Pb age for the
771 tuff before the Luoping biota and its geological implication. *Geological Review*, **59**, 159-164, in
772 Chinese with English abstract.
- 773 XU, X., LIU, B. & ZHAO, Y. (1996) Sequence Boundary Genesis and Basin-Mountain Transformation on
774 the Western Margin of the Upper Yangtze Platform during the Permian to Triassic. *Sedimentary*
775 *Geology and Tethyan Geology*, 1-30, in Chinese with English abstract.
- 776 XU, X., LIU, B., ZHAO, Y. & LU, Y. (1997) *Sequence Stratigraphy and Basin- Mountain Transformation*
777 *in the Western Margin of Upper Yangtze Lnadmass during the Permian to Triassic*. Geological
778 Publishing House, Beijing, 1-124pp, in Chinese with English abstract.
- 779 XU, Y., HE, B., CHUNG, S., MENZIES, M.A. & FREY, F.A. (2004) Geologic, geochemical, and geophysical
780 consequences of plume involvement in the Emeishan flood-basalt province. *Geol*, **32**, 917.
- 781 XU, Y., LUO, Z., HUANG, X., HE, B., XIAO, L., XIE, L. & SHI, Y. (2008) Zircon U - Pb and Hf isotope
782 constraints on crustal melting associated with the Emeishan mantle plume. *Geochimica et*
783 *Cosmochimica Acta*, **72**, 3084-3104.
- 784 XU, Z., HOU, L. & WANG, Z. (1992) *Orogenic Processes of the Songpan- Garze Orogenic Belt of China*.
785 Geol. Publ. House, Beijing.
- 786 YAN, D., ZHOU, M., LI, S. & WEI, G. (2011) Structural and geochronological constraints on the
787 Mesozoic-Cenozoic tectonic evolution of the Longmen Shan thrust belt, eastern Tibetan Plateau.
788 *Tectonics*, **30**, n/a-n/a.
- 789 YAN, Q., WANG, Z., LIU, S., SHI, Y., LI, Q., YAN, Z., WANG, T., WANG, J., ZHANG, D. & ZHANG, H.
790 (2006) Eastern Margin of the Tibetan Plateau A Window to Probe the Complex Geological History
791 from the Proterozoic to the Cenozoic Revealed by SHRIMP Analyses. *Acta Geologica Sinica*, **80**,
792 1285-1294, in Chinese with English abstract.

793 YIN, A. (1996) A Phanerozoic palinspastic reconstruction of China and its neighboring regions, in:
794 Tectonic Evolution of Asia.

795 ZHANG, G.W., MENG, Q.R. & LAI, S.C. (1995) Tectonics and structure of Qinling orogenic belt. *Science*
796 *in China*, **38**, 1379-1394.

797 ZHANG, Y., TANG, X.D., ZHANG, K., ZENG, L. & GAO, C. (2014) U - Pb and Lu - Hf isotope systematics
798 of detrital zircons from the Songpan - Ganzi Triassic flysch, NE Tibetan Plateau: implications for
799 provenance and crustal growth. *International Geology Review*, **56**, 29-56.

800 ZHANG, L., DING, L., PULLEN, A. & KAPP, P. (2015) Reply to comment by W. Liu and B. Xia on “Age
801 and geochemistry of western Hoh-Xil-Songpan-Ganzi granitoids, northern Tibet: Implications for
802 the Mesozoic closure of the Paleo-Tethys ocean” . *Lithos*, **212-215**, 457-461.

803 ZHANG, Y., JIA, D., SHEN, L., YIN, H., CHEN, Z., LI, H., LI, Z. & SUN, C. (2015) Provenance of detrital
804 zircons in the Late Triassic Sichuan foreland basin: constraints on the evolution of the Qinling
805 Orogen and Longmen Shan thrust-fold belt in central China. *International Geology Review*, **57**,
806 1806-1824.

807 ZHAO, J. & ZHOU, M. (2007) Geochemistry of Neoproterozoic mafic intrusions in the Panzhihua district
808 (Sichuan Province, SW China): Implications for subduction-related metasomatism in the upper
809 mantle. *Precambrian Research*, **152**, 27-47.

810 ZHAO, J., CHEN, Y. & LI, Z. (2006) Zircon U-Pb SHRIMP Dating for the Kangding Complex and Its
811 Geological Significance. *Geoscience*, **20**, 378-385, in Chinese with English abstract.

812 ZHAO, Y., XU, X. & LIU, B. (1996) High-frequency sequences and sea-level oscillations in the Emei area
813 on the western margin of the Upper Yangtze Platform. *Lithofacies Paleogeography*, **16**, 1-18, in
814 Chinese with English abstract.

815 ZHAO, Z., ZHOU, H., CHEN, X., LIU, Y., ZHANG, Y., LIU, Y. & YANG, Y. (2012) Sequence lithofacies
816 paleogeography and favorable exploration zones of the Permian in Sichuan Basin and adjacent areas,
817 China. *Acta Petrolei Sinica*, **33**, 35-51, in Chinese with English abstract.

818 ZHENG, L., YANG, Z., TONG, Y. & YUAN, W. (2010) Magnetostratigraphic constraints on two - stage
819 eruptions of the Emeishan continental flood basalts. *Geochemistry Geophysics Geosystems*, **11**.

820 ZHENG, Y., LI, H., SUN, Z., WANG, H., ZHANG, J., LI, C. & CAO, Y. (2016) New geochronology
821 constraints on timing and depth of the ancient earthquakes along the Longmen Shan fault belt,
822 eastern Tibet. *Tectonics*.

823 ZHOU, M., MA, Y., YAN, D., XIA, X., ZHAO, J. & SUN, M. (2006a) The Yanbian Terrane (Southern
824 Sichuan Province, SW China): A Neoproterozoic arc assemblage in the western margin of the
825 Yangtze Block. *Precambrian Research*, **144**, 19-38.

826 ZHOU, M., YAN, D., KENNEDY, A.K., LI, Y. & DING, J. (2002b) SHRIMP U - Pb zircon geochronological
827 and geochemical evidence for Neoproterozoic arc-magmatism along the western margin of the
828 Yangtze Block, South China. *Earth and Planetary Science Letters*, **196**, 51-67.

829 ZHOU, M., YAN, D., WANG, C., QI, L. & KENNEDY, A. (2006b) Subduction-related origin of the 750 Ma
830 Xuelongbao adakitic complex (Sichuan Province, China): implications for the tectonic setting of
831 the giant Neoproterozoic magmatic event in South China. *Earth and Planetary Science Letters*, **248**,
832 286-300.

833 ZHOU, M.F., KENNEDY, A.K., SUN, M., MALPAS, J. & LESHNER, C.M. (2002a) Neoproterozoic arc -
834 related mafic intrusions along the northern margin of South China: implications for the accretion of
835 Rodinia. *The Journal of geology*, **110**, 611-618.

836 ZHU, H., ZHOU, B., WANG, S., LUO, M., LIAO, Z. & GUO, Y. (2011) Detrital zircon U-Pb dating by LA-
837 ICP-MS and its geological significance in western margin of Yangtze terrane. *Journal of*
838 *Mineralogy and Petrology*, **31**, 70-74, in Chinese with English abstract.

839 ZHU, M., CHEN, H., ZHOU, J. & YANG, S. (2017) Provenance change from the Middle to Late Triassic of
840 the southwestern Sichuan basin, Southwest China: Constraints from the sedimentary record and its
841 tectonic significance. *Tectonophysics*, **700-701**, 92-107.

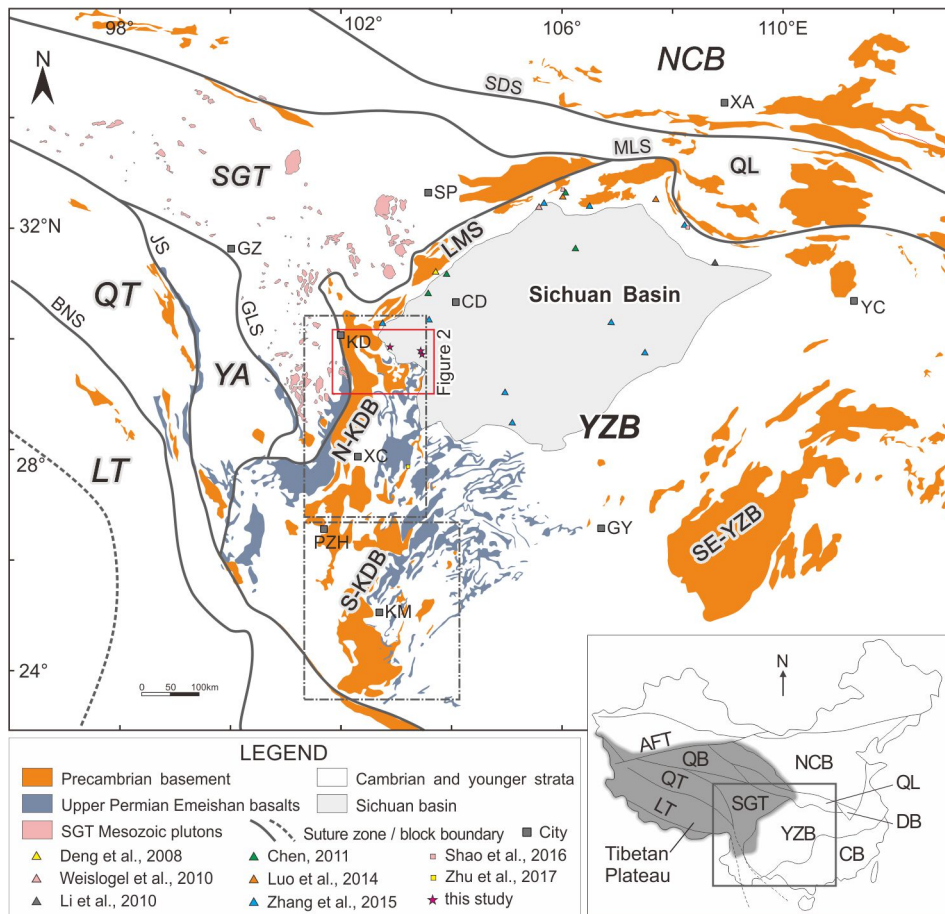
842 ZHU, Z. & WANG, G. (1986) Paleogeography of before and after deposition of green-bean rock (altered
843 tuff) between the early and middle Triassic in the upper Yangtze platform and its adjacent areas.
844 *Oil & Gas Geology*, **7**, 344-355, in Chinese with English abstract.

845

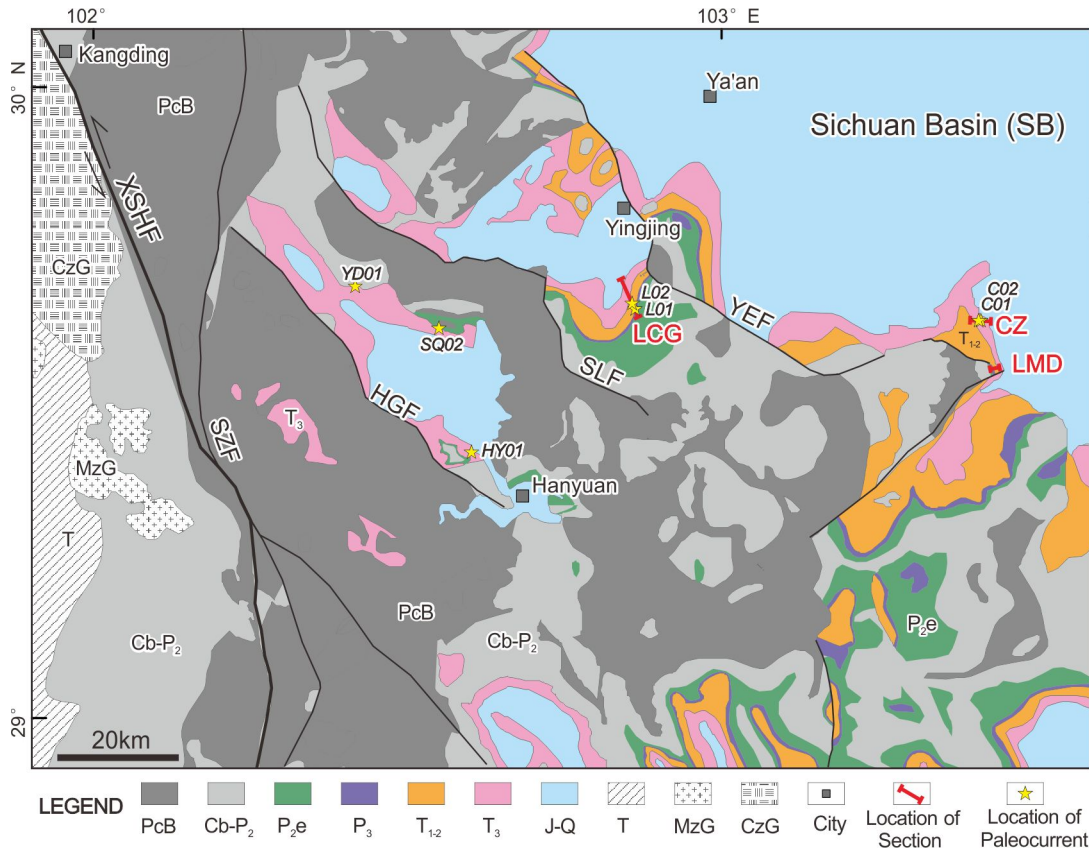
846

847

848



850
 851 **Fig. 1.** Simplified tectonic map of the Upper Yangtze Block and adjacent regions. Sites of previous
 852 detrital zircon geochronology studies of the Sichuan Basin are shown in the figure. Inset shows main
 853 tectonic elements of China. ATF, Altyn Tagh fault; CB, Cathaysia Block; CD, Chengdu; DB, Dabie
 854 orogen; GLS, Ganzi-Litang suture; GY, Guiyang; GZ, Ganzi; JS, Jinshajiang suture; KM, Kunming; LT,
 855 Lhasa terrane; MLS, Mianlue suture; N-KDB, Northern Kangdian basement; NCB, North China Block;
 856 PZH, Panzhihua; QB, Qaidam Block; QL, Qinling orogen; QT, Qiangtang terrane; S-KDB, Southern
 857 Kangdian basement; SDS, Shangdan suture; SGT, Songpan-Ganzi terrane; SP, Songpan; XA, Xi'an; XC,
 858 Xichang; YC, Yichang; YA, Yidun arc; YZB, Yangtze Block. Modified from Tian *et al.* (2012a) and
 859 Wang & Pan, (2013). The distribution of the Upper Permian Emeishan basalts is modified from Xu *et*
 860 *al.* (2004).
 861

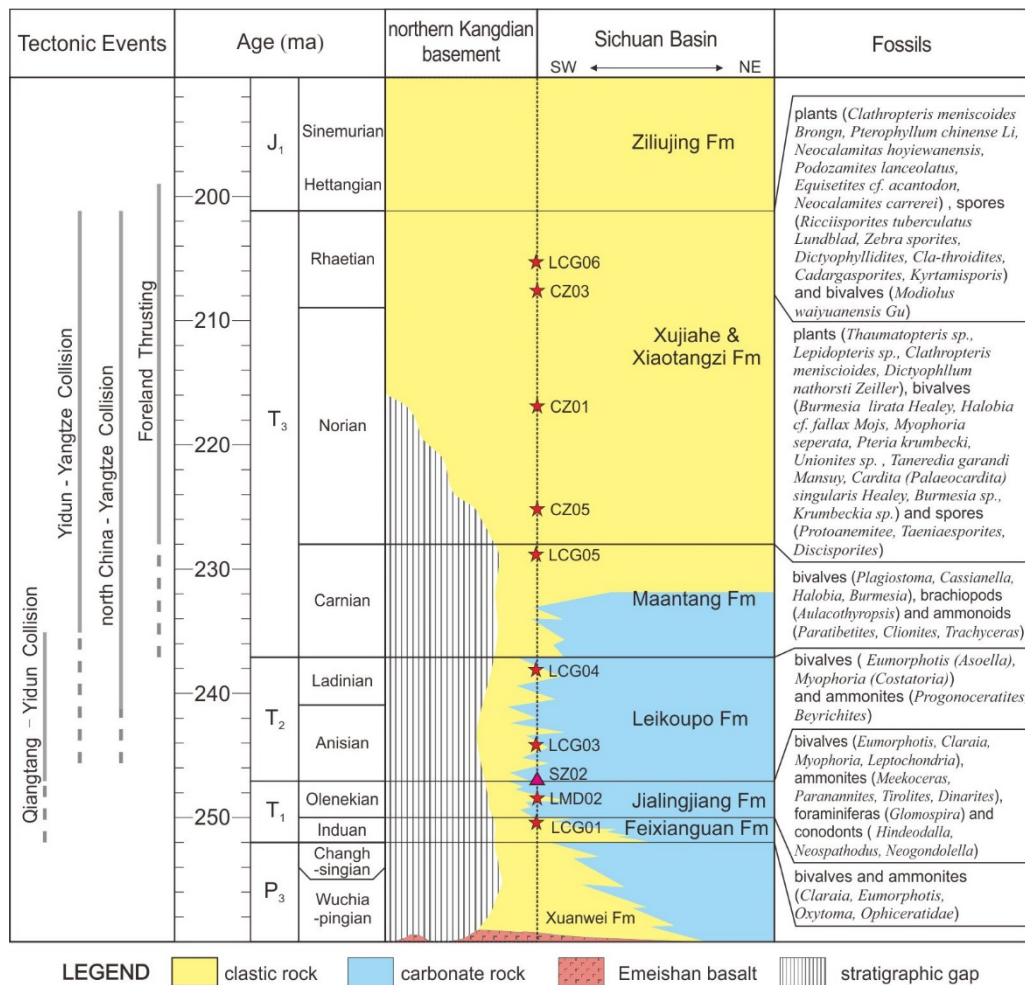


862

863 **Fig. 2.** Generalized geological map of the study area, modified from BGSP (1974). The location is shown
 864 in Fig. 1. Abbreviations: PcB — Precambrian Basement; Cb-P₂ — Cambrian - Middle Permian; P_{2e} —
 865 Upper Permian Emeishan basalts; P₂ — Upper Permian Xuanwei Formation; T₁₋₂ — Lower and Middle
 866 Triassic; T₃ — Upper Triassic; J-Q — Jurassic to Quaternary; T — Triassic in the eastern Songpan-Ganzi
 867 terrane; CzG — Cenozoic Granite; HGF — Hanyuan-Ganluo fault; MzG — Mesozoic Granite; SLF —
 868 Sanhe-Leibo fault; SZF — Shimian-Zhaojue fault; XSHF — Xianshuihe fault; YEF — Yingjing-Emei
 869 fault. Red solid lines and text makes the localities of the Longcanggou (LCG), Chuanzhu (CZ) and
 870 Longmendong (LMD) sections, from which samples were collected.

871

872



873

LEGEND clastic rock carbonate rock Emeishan basalt stratigraphic gap

874

Fig. 3. Stratigraphic nomenclature, age of the southern Sichuan Basin and northern Kangdian Oldland.

875

The time of foreland thrusting is after Zhang *et al.* (1995), Yin (1996); Meng, & Zhang (2000), Li *et al.*

876

(2003); the time of Yidun - Yangtze collision is after Reid *et al.* (2005), Roger *et al.* (2008), Yuan *et al.*

877

(2010), Wang *et al.* (2013); the time of Qiangtang- Yidun collision is after Reid *et al.* (2005), Pullen *et al.*

878

(2008), Roger *et al.* (2008), Roger *et al.* (2010). Time scale is from Gradstein *et al.* (2012). P₃ — the

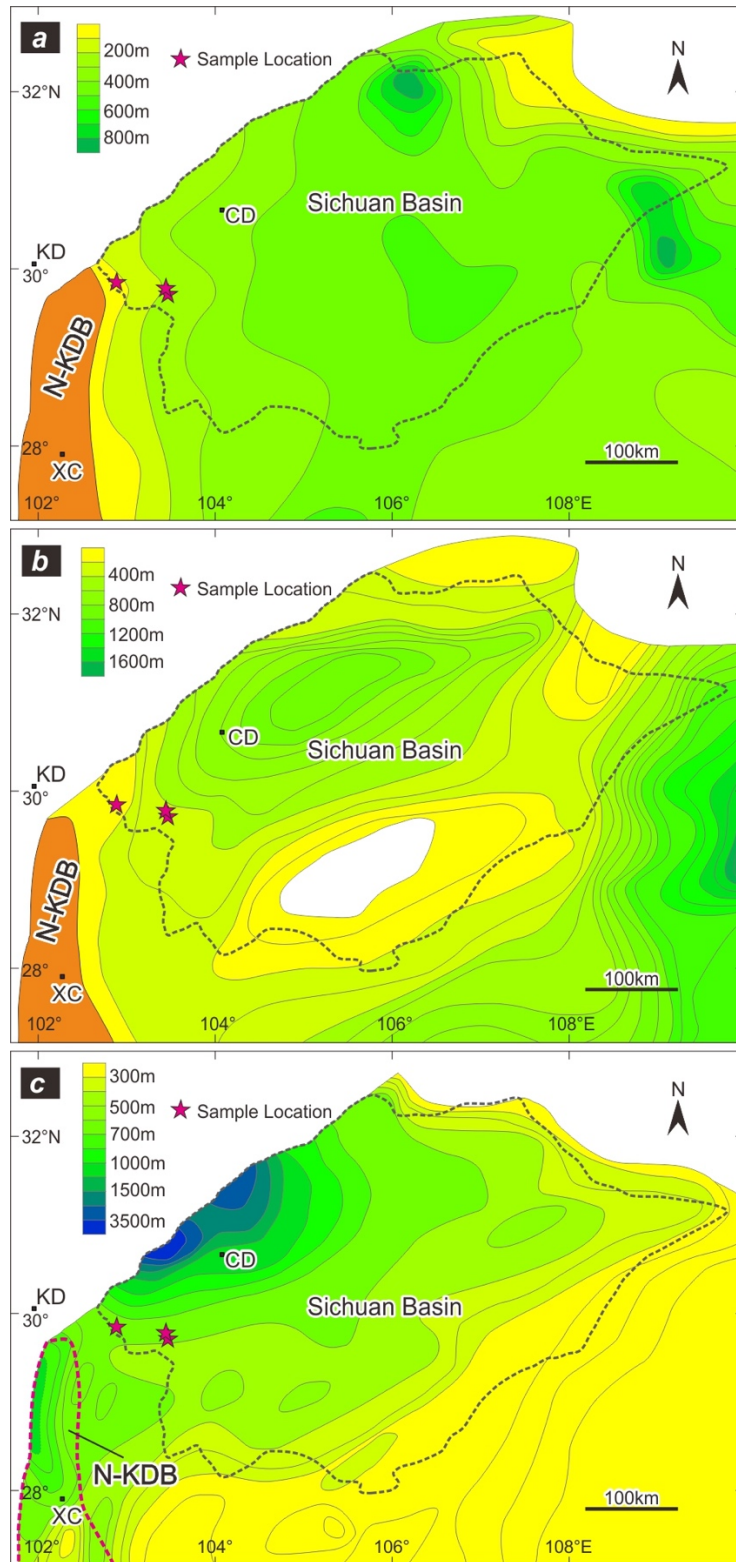
879

Late Permian; T₁ — the Early Triassic; T₂ — the Middle Triassic; T₃ — the Late Triassic; J₁ — the Early

880

Jurassic.

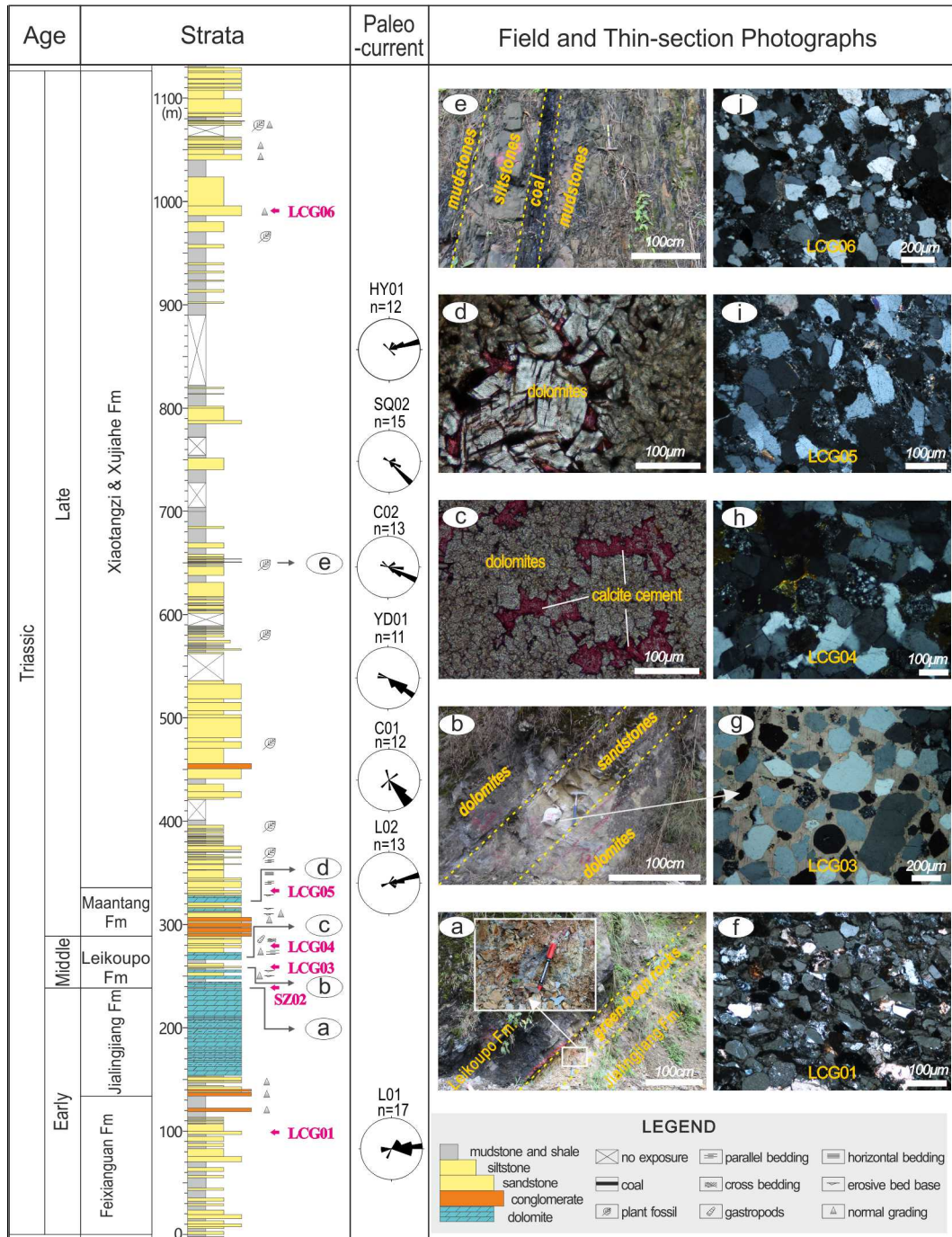
881



882

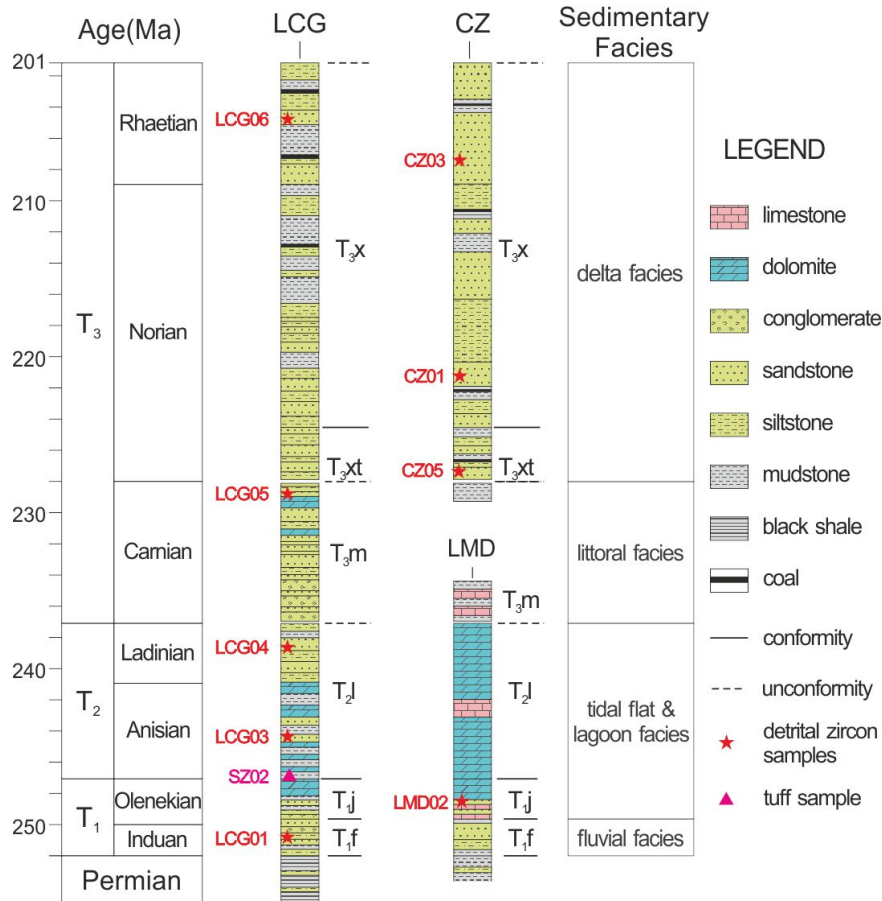
883 **Fig. 4.** The isopach of the Lower Triassic Feixianguan (a), Middle Triassic Leikoupo (b) and upper
 884 Triassic Xujiahe (c) formations in the Upper Yangtze Block, including the Sichuan Basin and
 885 surrounding regions (modified after Guo et al. 1996). Abbreviations for towns: CD = Chengdu, CQ =
 886 Chongqing, KD = Kangding, XC = Xichang. Note that at late Triassic time, the northern Kangdian
 887 basement (N-KDB) was inverted into a depocenter from erosion.

888



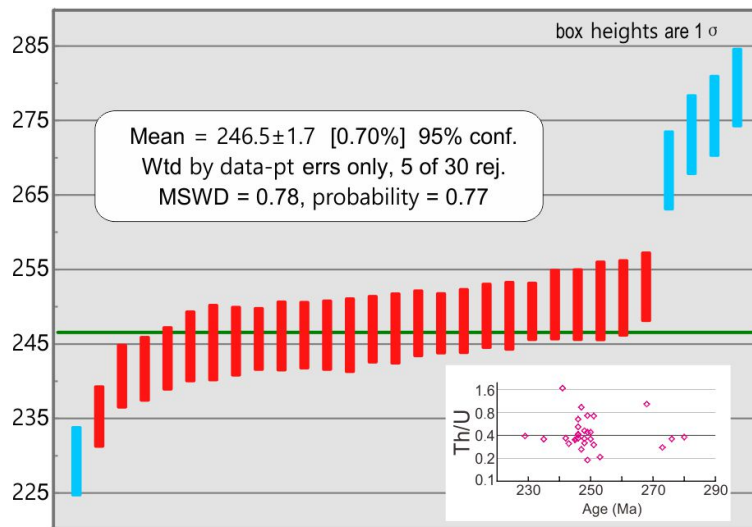
889

890 **Fig. 5.** Stratigraphy, rose diagrams of paleocurrent and thin-sections for the Longcanggou section. The
 891 locations of paleocurrent measurements are shown in Fig. 2. (a) Boundary (the “ altered tuff”) between
 892 the Lower Triassic Jialingjiang Formation and Middle Triassic Leikoupo Formation; (b) Dolomites
 893 interbedded between sandstones (sample LCG03); (c) Thin-section photograph of dolomites from the
 894 Leikoupo Formation; (d) Dolomites from the upper Mantang Formation; (e) Siltstones and mudstones
 895 interbedded with coal from upper part of Xujiache Formation; (f, g, h, i, and j) Thin-sections of sandstone
 896 from the LCG01, LCG03, LCG04, LCG05 and LCG06, collected from the Feixianguan (LCG01),
 897 Leikoupo (LCG03, LCG04), Mantang (LCG05) and Xujiache (LCG06) Formations.
 898



899
 900
 901
 902
 903
 904
 905
 906
 907

Fig. 6. Comparison of Triassic stratigraphy in the southwestern Sichuan Basin. CZ (Chuanzhu) section is compiled from [WGCMSPIB \(1984\)](#) and LMD (Longmendong) section from [Lin *et al.* \(1982\)](#), [Xu *et al.* \(1997\)](#) and [BGMRSB \(1997\)](#), with the sedimentary facies after [Zhao *et al.* \(1996\)](#); T_{1f} — Feixianguan Formation; T_{1j} — Jialingjiang Formation; T_{2l} — Leikoupo Formation; T_{3m} — Maantang Formation; T_{3xt} — Xiaotangzi Formation; T_{3x}—Xujiahe Formation; T₁—the Early Triassic; T₂—the Middle Triassic; T₃— the Late Triassic. Time scale is from the [Gradstein *et al.* \(2012\)](#), which is consistent with the tuff results derived from the sample SZ02 from the Longchanggou (LCG) section (see Fig. 7).

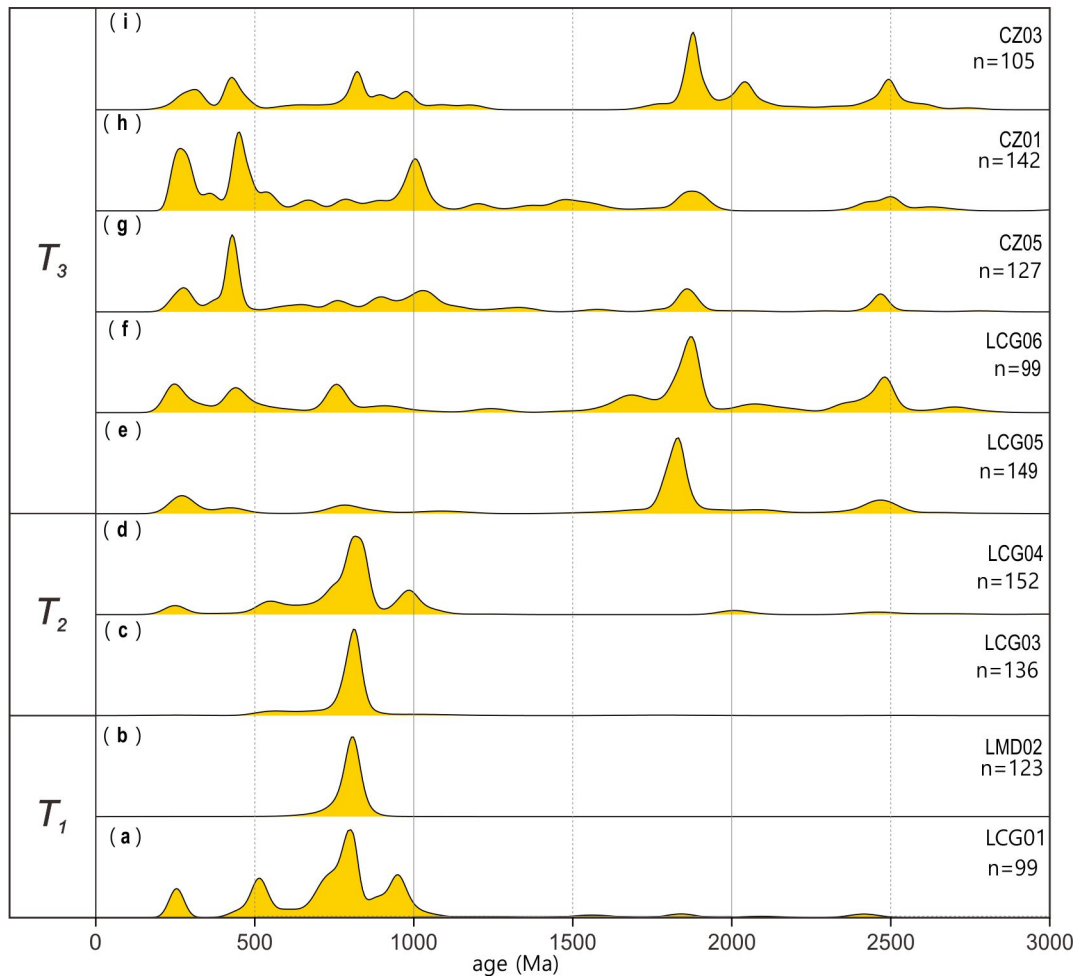


908
 909

Fig. 7. U–Pb zircon ages of the altered tuff (sample SZ02 this study). Blue dates are rejected by

910 ISOPLOT for calculating the weighted mean age.

911

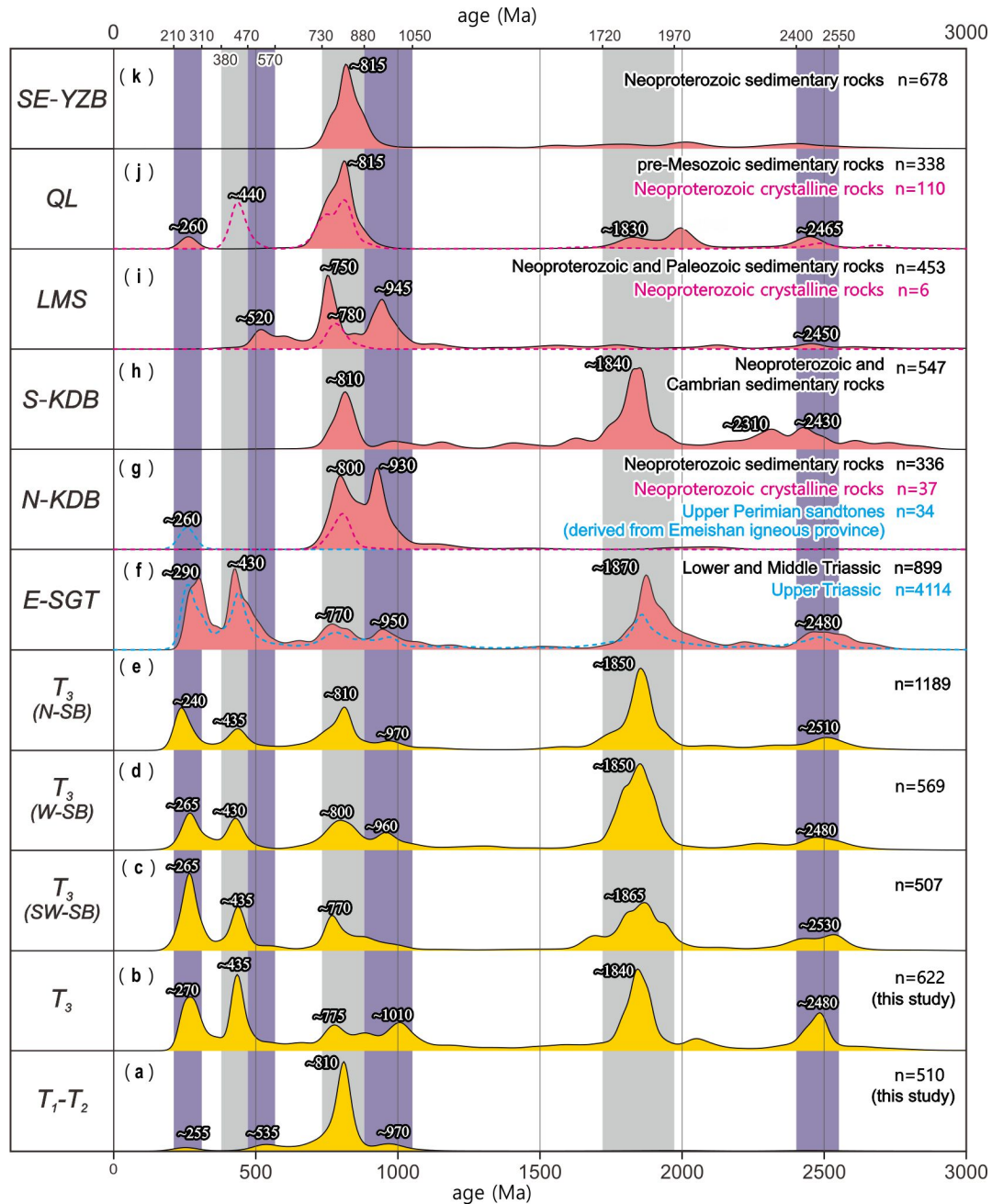


912

913 **Fig. 8.** Kernel Density Estimation (KDE) plots of the detrital zircon U-Pb data for samples LCG01,
914 LMD02, LCG03, LCG04, LCG05, LCG06, CZ05, CZ01 and CZ03, respectively. T₁, T₂ and T₃ are Early,
915 Middle and Late Triassic, respectively.

916

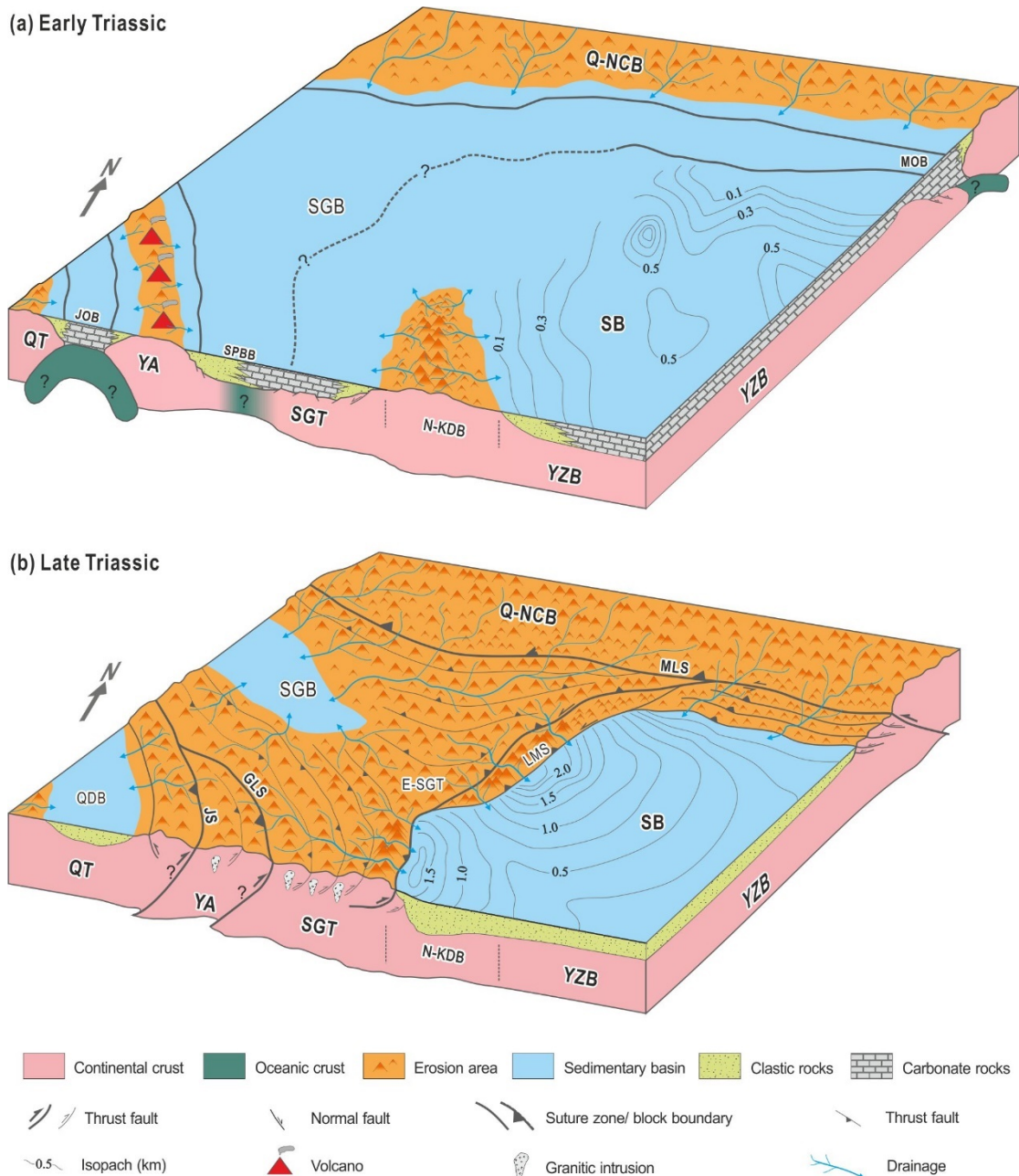
917



918

919 **Fig. 9.** KDE plots for the detrital zircon ages of the Triassic sediments of the Sichuan Basin and potential
 920 source areas. (a-b) Age spectra of the Lower-Middle and Upper Triassic sediments in the southwestern
 921 Sichuan Basin. (c-e) Spectra of the Upper Triassic sediments in the southwestern, western and northern
 922 Sichuan Basin, reported in previous studies (Deng *et al.*, 2008; Weislogel *et al.*, 2010; Chen, 2011; Luo
 923 *et al.*, 2014; Zhang *et al.*, 2015; Shao *et al.*, 2016; Zhu *et al.*, 2017). Spectra of potential areas, including
 924 (f) E-SGT (eastern Songpan-Ganzi terrane), compiled from the Lower-Middle Triassic sedimentary rocks
 925 (black solid line) (Weislogel *et al.*, 2006, 2010; Enkelman, 2007; Ding *et al.*, 2013; Wang *et al.*, 2013)
 926 and the Upper Triassic sedimentary rocks (blue dash line) (Wang *et al.*, 2007; Weislogel *et al.*, 2006,
 927 2010; Ding *et al.*, 2013; Wang *et al.*, 2013; Zhang *et al.*, 2014,2015), (g) N-KDB (northern Kangdian
 928 Basement), compiled from both crystalline (red dash line) (Roger & Calassou, 1997; Guo *et al.*, 1998;
 929 Shen *et al.*, 2000; Li *et al.*, 2001; Li *et al.*, 2002; Zhou *et al.*, 2002b; Shen *et al.*, 2003; Li *et al.*, 2003b;
 930 Zhou *et al.*, 2006a; Lin *et al.*, 2006b; Yan *et al.*, 2006; Zhao *et al.*, 2006; Geng *et al.*, 2007; Huang *et al.*,

931 2009; Lin, 2010; Ruan, 2013; Meng *et al.*, 2015) and sedimentary rocks (black solid line) (Zhou *et al.*,
 932 2006a; He *et al.*, 2007; Sun *et al.*, 2009), (h) S-KDB (southern Kangdian Basement), compiled from
 933 sedimentary rocks (Sun *et al.*, 2009; Wang *et al.*, 2012), (i) LMS (Longmen Shan thrust belt), compiled
 934 from both crystalline (red dash line) (Zhou *et al.*, 2006b; Meng *et al.*, 2015) and sedimentary rocks (black
 935 solid line) (Duan *et al.*, 2011; Chen *et al.*, 2016), (j) QL (Qinling orogen), compiled from both crystalline
 936 (red dash line) (Li *et al.*, 2016 and references therein) and sedimentary rocks (black solid line) (He *et al.*,
 937 2007; Wang *et al.*, 2013a), (k) SE-YZB (southeastern Yangtze Block), compiled from sedimentary rocks
 938 (Wang *et al.*, 2010; Wang & Zhou, 2012).
 939
 940
 941



942
 943 **Fig. 10.** Models for Triassic tectonic evolution of the Upper Yangtze Block and its link to adjacent
 944 structural belts. E-SGT, Eastern Songpan-Ganzi terrane; GLS, Ganzi-Litang suture; JOB, Jinshajiang

945 Ocean Basin; JS, Jinshajiang suture; LMS, Longmen Shan thrust belt; LSB, Longmen Shan basement;
946 MLS, Mianlue suture; MOB, Mianlue Ocean Basin; N-KDO, Northern Kangdian basement; QDB,
947 Qamdo Basin; Q-NCB, Qingling Terrane and Northern China Block; QT—Qiangtang terrane; SB,
948 Sichuan Basin; SE-SGT, eastern Songpan-Ganzi terrane; SGB, Songpan-Ganzi Basin; SGT— Songpan-
949 Ganzi terrane; SPBB, Songpan back arc Basin; YA—Yidun arc. The tectonic evolution between
950 Qiangtang terrane and northern Kangdian basement is after Roger *et al.* (2008)
951
952